Hindawi Publishing Corporation
Advances in Meteorology
Volume 2010, Article ID 319138, 24 pages
doi:10.1155/2010/319138

Research Article

Simulation of Surface Ozone Pollution in the Central Gulf Coast Region Using WRF/Chem Model: Sensitivity to PBL and Land Surface Physics

Anjaneyulu Yerramilli,[1] Venkata Srinivas Challa,[2] Venkata Bhaskar Rao Dodla,[1] Hari Prasad Dasari,[3] John H. Young,[1] Chuck Patrick,[1] Julius M. Baham,[1] Robert L. Hughes,[1] Mark G. Hardy,[1] and Shelton J. Swanier[1]

[1] *Trent Lott Geospatial and Visualization Research Centre, Jackson State University, 1230 Raymond Road, Jackson, MS 39217-204, USA*
[2] *Radiological Safety Division, Indira Gandhi Centre for Atomic Research, Kalpakkam 603102, India*
[3] *Centro de Geophysica de Evora, University of Evora, Evora, Portugal*

Correspondence should be addressed to Anjaneyulu Yerramilli, yerramilli.anjaneyulu@jsums.edu

Received 19 January 2010; Revised 10 June 2010; Accepted 4 August 2010

Academic Editor: Bert Holtslag

The fully coupled WRF/Chem (Weather Research and Forecasting/Chemistry) model is used to simulate air quality in the Mississippi Gulf coastal region at a high resolution (4 km) for a moderately severe summer ozone episode between 18 CST 7 and 18 CST 10 June 2006. The model sensitivity is studied for meteorological and gaseous criteria pollutants (O_3, NO_2) using three Planetary Boundary Layer (PBL) and four land surface model (LSM) schemes and comparison of model results with monitoring station observations. Results indicated that a few combinations of PBL and LSMs could reasonably produce realistic meteorological fields and that the combination of Yonsei University (YSU) PBL and NOAH LSM provides best predictions for winds, temperature, humidity and mixed layer depth in the study region for the period of study. The diurnal range in ozone concentration is better estimated by the YSU PBL in association with either 5-layer or NOAH land surface model. The model seems to underestimate the ozone concentrations in the study domain because of underestimation of temperatures and overestimation of winds. The underestimation of NO_2 by model suggests the necessity of examining the emission data in respect of its accurate representation at model resolution. Quantitative analysis for most monitoring stations indicates that the combination of YSU PBL with NOAH LSM provides the best results for various chemical species with minimum BIAS, RMSE, and high correlation values.

1. Introduction

Air quality in the Central Gulf Coastal region covering Mississippi, Alabama, and Louisiana in the southeast US is affected by high ozone levels during summer season. Summer Ozone (one of the EPA criteria pollutants of major significance, mainly formed by the oxidation process of volatile organic compounds (VOCs) in the presence of NOx (NO and NO_2) and SO_2 and formation driven by the sunlight intensity) episodes are some air quality concerns as considerable number of anthropogenic and biogenic sources in this area contribute to precursors of ozone in this region. Occurrence of gulf breeze (sea-land breeze), prevailing high pressure systems over mid-south or Gulf of Mexico, westerly winds and associated meteorological processes are attributed to cause high ozone levels in this coastal region [1]. A key factor leading to the incidence of high ozone concentrations in the coastal areas of Mississippi is the gulf breeze, a shallow wind system that develops as a result of differential heating of the land and water surfaces. Yerramilli et al. [2] and Challa et al. [3, 4] have conducted a few studies on air quality from this region focusing on observational and modeling aspects of mesoscale flows, plume dispersion from elevated point sources and the sensitivity of dispersion simulations to meteorological fields. Air quality/dispersion modeling in complex geographical regions as in Mississippi Gulf coastal area requires at least an accurate representation of the meteorological fields to understand various phenomena such as transport, diffusion, transformation and removal of air pollutants. Also the sources and sinks should be well included.

Several studies on air quality, environmental planning, and emission management research used meteorological model predictions for understanding air quality episodes (namely, Byun et al. [5], Sistla et al. [6], Mao et al. [7], Zhang et al. [8], Otte et al. [9], among others). Simulations from air quality models depend on a number of important factors including meteorological conditions at the scale of study. Meteorological quantities that directly influence the air quality simulations include wind field, temperature profiles, water vapor mixing ratio, atmospheric stability, boundary layer depth, turbulent fluxes, surface pressure, clouds, shortwave radiation in the lowest 2 or 3 km [7, 10, 11] of the troposphere and surface precipitation. Several parameters in a meteorological model influence its performance, which include the model initial conditions, physical process parameterizations and spatial and temporal resolutions [12–16]. Often the study regions cover smaller areas or complex topography where the model performance needs to be improved by application of available data on the atmospheric state and better representation of physical processes [17]. Hence improved prediction of atmospheric variables is a challenging issue to obtain accurate air quality estimates.

Of the various atmospheric physical processes, the land surface and planetary boundary layer processes are interactive and play important roles in the simulation of the lower atmospheric turbulence, winds and other state variables. The land surface model (LSM) calculates the heat and moisture fluxes over land, sea-ice points and provide a lower boundary condition for the vertical transport in the PBL [18]. The development and growth of the PBL depends on the surface heat and moisture fluxes, their upward mixing by the turbulent eddies and subsidence. All of these phenomena influence the atmospheric transport and diffusion processes and hence are important in air quality modeling. Thus it is important to evaluate model performance for identification of a physically reasonable combination of land surface and PBL schemes for air quality simulations. Several studies focused on meteorological model evaluations within the scope of air quality modeling [7, 8, 12, 19, 20]. Many of these evaluation studies are based on the Pennsylvania State University/National Center for Atmospheric Research (PSU/NCAR) mesoscale model MM5 which is used as a meteorological driver for air quality models. For example, Berg and Zhong [16] compared MM5 simulations using three PBL schemes (Blackadar, MRF and Gayno-Seaman) and reported relatively better performance with first-order Blackadar PBL scheme which produced better comparisons with observed PBL heights than the TKE-based schemes. Hanna and Yang [21] performed evaluations for the simulation of near surface winds, temperature gradients and mixing depths with several mesoscale models and reported that the typical root-mean-square error (rmse) for hourly outputs is about 2-3 ms^{-1} for wind speed, 50 degrees for wind direction, and that the simulated daytime mixing depths are within 20% of observations. Steeneveld et al. [22] evaluated the ability of three mesoscale models (i.e., MM5, COAMPS, and HIRLAM) for the representation of diurnal cycle of the atmospheric boundary layer using experimental observations. Their study reported that in all the models the amplitude of the temperature cycle and wind speed are underestimated, stable boundary layer height is overestimated for windy conditions, and the stratification of nighttime surface inversions is underestimated.

Zhang and Zheng [23], compared results of MM5 simulations with first order non-local Blackadar, first order eddy diffusion scheme MRF and three TKE closure schemes (Mellor-Yamada-Janjic, Burk-Thomson and Gayno-Seaman). They reported large deviations in the near-surface temperature and wind speed from different simulations and that Blackadar provided closer comparisons than the others. Bright and Mullen [24] reported that the Blackadar and MRF schemes better simulated the PBL structure and its height compared to the TKE schemes.

The meteorological and chemical processes are usually separated in the offline air quality models such as CMAQ, and CAMX, where the meteorological fields are first predicted using an atmospheric dynamical model at a certain spatial and time interval, which is then interpolated in time and space to the air quality model. This offline approach has certain limitations such as loss of atmospheric information, absence of feedback mechanism between chemical and atmospheric processes and different physical parameterizations in the meteorological and air quality modules. In reality both meteorological and chemical processes interact in the atmosphere. For instance clouds affect the photolysis rates and thus the formation of chemical species which may influence the radiation thus influence the formation of photochemical species. Recently a next generation online air quality model WRF/Chem [25] has been developed with full integration of the meteorological and chemistry modules which use the same computational grid and same physical parameterizations and includes the feedback between the chemistry and physical processes. The meteorological model of WRF/Chem is the Advanced Research Weather Research and Forecasting (ARW) model developed by NCAR. Relatively few studies exist on the performance of the WRF and its online chemistry version WRF/Chem [25] for air quality studies (e.g., [3, 26–31]). Borge et al. [29] conducted an extensive sensitivity analysis of WRF2.2 for two air pollution episodes in Iberian Peninsula and identified a suitable configuration of physics parameterizations for better predictions of winds, temperature and humidity fields. However their study is limited to the evaluation of meteorological predictions with respect to different available physics schemes. De Foy et al. [31] evaluated the WRF model for the complex wind flows in the Mexico City basin area with data from field campaigns using statistical techniques, cluster analysis of flow trajectories and concentration measurements. In a sensitivity study with WRF/Chem over the Houston-Galveston area Misenis et al.

[28] reported that the meteorological schemes affected the chemical predictions and that the combination of Yonsei University (YSU) PBL scheme with NOAH LSM produced better results for ozone and PM2.5 than other available combinations. Zhang et al. [32] studied the air quality over Mexico City using WRF/Chem simulations and reported that the model performs much better during daytime than nighttime for both chemical species and meteorological variables and different combinations of the available PBL and land surface schemes did not reduce the errors.

The present work is a contribution to the evaluation of the WRF/Chem online chemistry model with a focus on its application to air quality studies in the Mississippi Gulf Coastal region. The objective of this work is to evaluate the model performance for both meteorological and chemical species and study the sensitivity with different PBL and land surface physics options. Qualitative and quantitative methods are followed to evaluate the model sensitivity and help reduce uncertainties in air quality simulations.

2. Methodology

2.1. Model Description. The Advanced Research WRF (ARW) mesoscale model version 3.1 with Eulerian mass solver developed by NCAR [18] is used in the present study. The model consists of fully compressible nonhydrostatic equations, terrain following vertical coordinate, and staggered horizontal grid. The model has multiple options for spatial discretization, diffusion, and nesting. It incorporates a number of parameterization schemes for subgrid scale physical processes. The physics consists of microphysics, cumulus convection, planetary boundary layer turbulence, land surface, longwave and shortwave radiation. The fully coupled chemistry within the WRF model, called WRF/Chem was developed at NOAA (National Oceanic and Atmospheric Administration) [25]. The chemistry module of WRF/Chem treats the processes of transport, wet and dry deposition, chemical transformation, photolysis, aerosol chemistry and dynamics. Both the meteorological and air quality components in WRF/Chem use the same transport scheme, the same horizontal and vertical grids, the same physics schemes and the same time step for transport and vertical mixing. The model incorporates several different chemistry, aerosol and photolysis schemes.

2.2. Simulation Period. Simulations using WRF/Chem in the study region are conducted for a summer synoptic condition in 18 CST 7 June–18 CST 10 June in the year 2006. The choice of the study cases is based on the analysis of air pollution records of the last few years from the region of interest and availability of meteorological and air pollution monitoring observations for model evaluation. A moderately severe air pollution episode with ozone formation (60 to 110 ppbv) occurred in the study region during the above period. The daily maximum 8-hour average ozone concentrations ranged between 67 and 84 ppbv at several monitoring stations during this period. A considerable number of stations had 8-hour average ozone concentrations just above 80 ppbv during the three-day period. Although this period does not characterize a very severe ozone episode, it is important as the 8-hour ozone values exceeded 60 ppbv, a threshold which can seriously affect people suffering from respiratory deficiencies. The study period represents a synoptic situation with weak pressure gradients, geostrophic winds of about 5 $\mathrm{ms^{-1}}$, diurnal air temperature of 18–35°C, relative humidity of 35%–85% conducive for the recirculation and accumulation of pollutants from land-sea breeze mesoscale flows over the Mississippi Gulf Coast.

2.3. Model Configuration and Initialization. The model is used with nested domains and at high resolution of 4 km. Three domains are used in the model, the outer domain covers a fairly large region of south-eastern U.S and the inner 3rd domain covers the Mississippi Gulf Coast and parts of Louisiana and Alabama states at 4km fine resolution (Figure 1). The model domains are centered at 32.8 N, −87.5 E with Lambert Conformal Conic (LCC) projection. The grid spacing is 36 km, 12 km and 4 km for the domains 1, 2 and 3, respectively. The grid sizes in the east-west and north-south directions in each domain are 56×42, 109×82 and 178×136, respectively. A total of 31 vertical levels with 10 levels in the lower atmospheric region (below 850 hPa) are considered in the model. This vertical resolution is chosen such that the model fairly captures the boundary layer turbulence structures and does not involve huge computational costs in the meteorology-chemistry coupled mode. The inner domains 2, 3 are two-way interactive. Terrain, land use and soil data are interpolated to the model grids from USGS global elevation, vegetation category data and FAO Soil data with suitable spatial resolution for each domain ($5'$, $2'$ and $30''$ for domains 1, 2 and 3, resp.) to define the lower boundary conditions. The dependent parameters are albedo, roughness length, thermal inertia, moisture availability and emissivity for land use and thermal diffusivity, available water capacity, wilting point moisture, and so forth, for soil category. The initial and lateral boundary conditions for WRF/Chem are defined from the National Centers for Environmental Prediction (NCEP) Final Analysis (FNL) data available at $1^\circ \times 1^\circ$ resolution and temporal resolution of 6 hours. The model is initialized with the above data at 18 CST 7 June 2006 and integrated for 72 hours up to 18 CST 10 June. The mesoscale model initialized with synoptic analysis takes certain amount of time, called the “spin up” period to adjust to the model topography and for the evolution of the mesoscale structures in the high-resolution domains. An initial 12-hour model integration period is used for spin-up for the simulations to be consistent with the mesoscale features of the respective domains.

The chemical parameterizations considered are the Regional Acid Deposition Model version 2 (RADM2) gas-phase chemical mechanism [33, 34] and Madronich photolysis scheme [35]. No aerosol module is included for the present study. The default profiles for chemical species available with the model are used as the initial pollutants at the start of the model since no previous day simulations are made. This approach to initialize the chemistry is used based on results from past studies [36–38] which indicate that the simulations are not very sensitive to the initial chemical conditions. The source for the anthropogenic emissions data is the US Environmental Protection Agency (EPA) National Emissions Inventory (NEI) 2005 inventory. This data consists of area-type emissions on a structured 4 km grid and point type emissions at latitude and longitude locations. The data is interpolated to model grids using the emissions processing program available with WRF/Chem. The biogenic emissions are calculated online using the Guenther scheme. This module treats the emissions of isoprene, monoterpenes, other volatile organic compounds (OVOC), and nitrogen emission by the soil [25]. The emission of isoprene by forests depends on both temperature and photosynthetic active radiation. In Guenther parameterization the isoprene emission rate are proportional to its rate at a standard temperature and a standard flux of photosynthetic active radiation. A radiation flux correction term and a temperature correction term for forest isoprene emissions is applied. The isoprene emissions of agricultural and grassland areas are considered to be functions of the temperature only. The above chemical options are chosen as they have yielded good results in previous studies.

There are several physics options available in WRF to represent PBL turbulence, land surface fluxes, microphysics, cumulus convection and atmospheric radiation. The model runs are conducted with the Lin et al. [39] microphysics, new Grell convective parameterization scheme for domains 1, 2. Atmospheric shortwave and longwave radiation components are computed using the Goddard scheme [40] and RRTM [40] scheme, respectively. A time interval of 36 s is used for calling the radiation schemes.

2.4. Sensitivity Experiments. The land surface and PBL parameterizations influence the simulation of winds, turbulence, and other state variables in the lower atmosphere where dispersion and transport of pollutants occurs. Several works addressed the impact of the PBL and LSM schemes on air quality modeling results (see Mao et al. [7], Fast and Zhong [37], De Foy et al. [38], among others). Most of these studies considered the PBL schemes available with MM5. Borge et al. [29] used three PBL schemes and three LSMs available in WRF V2.2 in addition to several other model physics options. However, of the two schemes used in their study the YSU is an updated version of the MRF scheme and they are conceptually similar. The present contribution uses three conceptually different PBL schemes and four LSMs available in WRF/Chem 3.1 combined meteorological and air quality modeling system for model sensitivity evaluation (Table 1). The options selected for vertical turbulent transports in PBL are Yonsei University (YSU) PBL scheme [41], Mellor-Yamada-Janjic (MYJ) scheme [41–43], and Asymmetrical Convective Model version 2 (ACM) PBL [44]. The YSU scheme is a modification to the MRF scheme [45] using an explicit treatment of entrainment rather than implicit. It is a non-local first-order scheme in which the vertical transfers are dependent on the bulk characteristics of the PBL and includes counter gradient transports of temperature, momentum arising from large-scale eddies. The eddy diffusivity coefficient for momentum is a function of the friction velocity and the PBL height, while those for temperature and moisture are computed using a Prandtl number relationship. An entrainment layer is explicitly calculated in the PBL top proportional to the surface buoyancy flux. The MYJ scheme includes a prognostic equation for turbulent kinetic energy (TKE), a level 2.5 turbulence closure approximation to determine eddy transfer coefficients and uses local vertical mixing within PBL [42, 43, 46]. The ACM is a combination of the high-resolution Blackadar model and an eddy diffusion model. It computes eddy diffusion in the stable and unstable conditions, both local and non-local transport in unstable conditions and is well suited for consistent PBL transports of various quantities. The friction velocity and the surface exchange coefficients for heat, moisture and momentum are calculated through the MM5 surface layer similarity theory [18] for the MRF and YSU schemes. The land-surface models (LSMs) use atmospheric information from the surface layer scheme together with the land-surface properties (defined by land use, soil type, etc.) to compute eddy heat and moisture transports in the PBL. Thus the nature of LSM directly influences the estimation of PBL height. Four well-suited LSM schemes available in WRF are chosen in the study. These are the 5-layer soil thermal diffusion (SOIL) model [47], the NOAH land surface model (NOAH) [48], Rapid Update Cycle (RUC) Model [49], and the Pleim-Xiu (PX) LSM [50, 51]. The 5-layer soil model solves the thermal diffusivity equation with 5 soil layers. The energy budget includes radiation, sensible and latent heat fluxes. It treats the snow-cover, soil moisture fixed with a land use and season-dependent constant value. The NOAH LSM is an improvement to the OSU LSM [48] and treats explicit soil and vegetation effects. It uses the time-dependent soil fields and uses a 4-layer soil temperature and moisture model with canopy moisture and snow-cover prediction. The RUC LSM has a high resolution soil model (6 layers) and includes the effects of vegetation, canopy water and snow. The Pleim-Xue LSM includes a 2-layer force-restore soil temperature and moisture model and considers evapotranspiration, soil evaporation, and evaporation from wet canopies. The PX is generally coupled to the ACM PBL. A set of 10 numerical experiments are conducted with different alternative PBL and LSM combinations (YSUSOIL, YSUNOAH, YSURUC, MYJSOIL, MYJNOAH, MYJRUC, ACMSOIL, ACMNOAH, ACMRUC and ACMPX) (Table 1).

2.5. Observational Datasets Used for Evaluation. The meteorological observations used for model evaluations include the NCEP Atmospheric Data Project (ADP) Global Upper air and Surface observation data set over the southeast United States, automated weather stations data over Louisiana from Louisiana Agri. Climatic Data Center (http://weather.lsuagcenter.com/) and surface reports, upper air soundings obtained from University of Wyoming (http://weather.uwyo.edu/). The NCEP ADP data set is obtained from the NCAR Research Data Archive (http://dss.ucar.edu/datasets/ds337.0). The model performance is studied mainly from the model fine grid nest (3rd domain) and all stations falling in

Table 1: Details of the grids and physics options used in the WRF/Chem model.

Dynamics		Primitive equation, nonhydrostatic	
Vertical resolution		31 levels	
Domains	Domain 1	Domain 2	Domain 3
Horizontal resolution	36 km	12 km	4 km
Grid points	54 × 40	109 × 76	187 × 118
Domains of integration	98.00°W–72.77°W 22.93°N–39.47°N	94.86°W –79.56°W 26.49°N –36.33°N	92.5°W–84.60°W 28.39°N–33.66°N
Radiation		Goddard scheme for short wave RRTM scheme for long wave	
Sea surface temperature		NCEP FNL analysis data	
Cumulus convection		New Grell scheme on the outer grids domain 1 and domain 2	
Explicit moisture		Lin scheme	
Sensitivity Experiments		PBL/Land Surface Scheme	
YSUSOIL		Yonsei University PBL, 5-layer soil diffusion model	
YSUNOAH		Yonsei University PBL, NOAH LSM	
YSURUC		Yonsei University PBL, RUC LSM	
MYJSOIL		Mellor-Yamada-Janjic PBL, 5-layer soil diffusion model	
MYJNOAH		Mellor-Yamada-Janjic PBL, NOAH LSM	
MYJRUC		Mellor-Yamada-Janjic PBL, RUC LSM	
ACMSOIL		Asymmetric Convective Model, 5-layer soil diffusion model	
ACMNOAH		Asymmetric Convective Model, NOAH LSM	
ACMRUC		Asymmetric Convective Model, RUC LSM	
ACMPX		Asymmetric Convective Model, Pleim-Xue LSM	

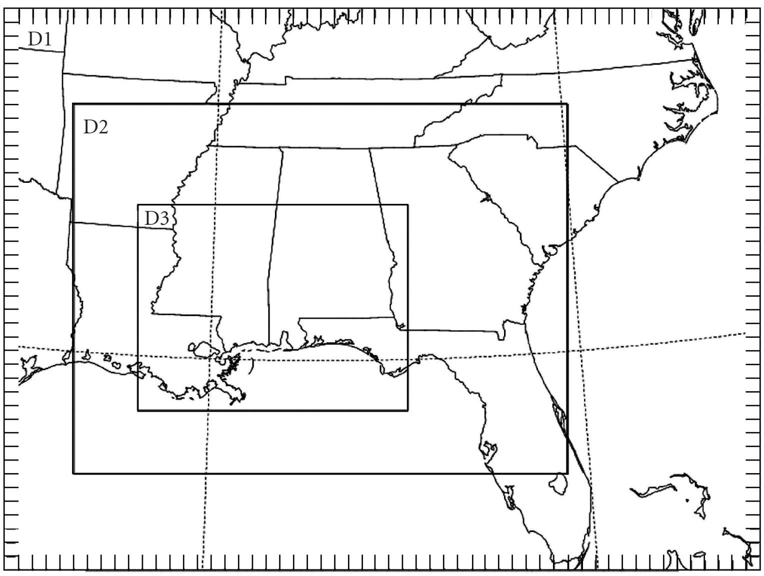

Figure 1: Modelling domains used in WRF/Chem. Outer domains D01, D02 are coarse with resolutions 36 and 12 km and the inner finer domain (D3) is of resolution 4 km.

this domain are considered for statistical analysis. The data from NCEP ADP consists of about 275 near-surface meteorological observations and 4 upper air soundings in the study region falling in model 3rd domain. The surface meteorological variables of temperature, humidity and winds are available four times a day at 00, 06, 12, and 18 CST while the upper air soundings are mostly available at 06 and 18 CST from ADP data sets. The pollutant species considered for WRF/Chem evaluations are NO_2 and O_3. As in the case of the meteorological results the model evaluation for chemical species focuses on the fine-grid domain. The observational databases include routine

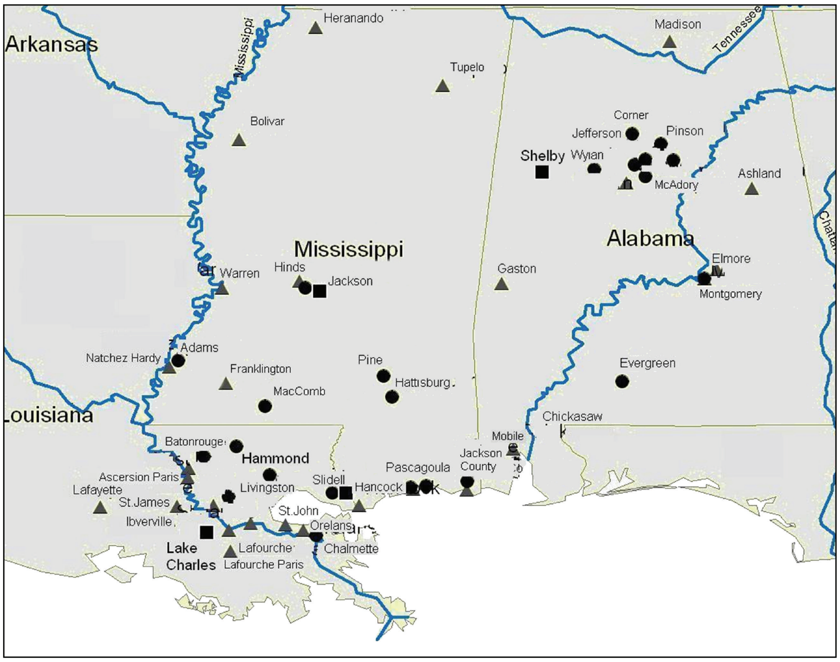

▲ Air quality monitoring stations
● Surface met. stations
■ Upper air met. stations

Figure 2: Location map of a few meteorological and air quality monitoring stations used in the sensitivity analysis.

monitoring networks such as the Aerometric Information Retrieval System (AIRS)-Air Quality System (AQS) (http://www.epa.gov/air/data/index.html) and Interagency Monitoring of Protected Visual Environments (IMPROVE) (http://vista.cira.colostate.edu/improve/). A total of 32 ground-based air quality monitoring stations spread in the 3rd domain are considered in the analysis of air quality predictions. Some of the stations used for visual comparisons of meteorological and air quality fields are shown in Figure 2.

2.6. Evaluation Methodology. Model evaluations included both visual comparisons and statistical analysis. The region up to 850 hPa level (~1.5 to 2 km above ground) is important as it covers the lower turbulent region in the atmosphere where vertical mixing and dilution of the pollutants occurs. Hence the surface and pressure levels 1000 hPa, 925 hPa, and 850 hPa are selected to assess the model performance. The comparisons from WRF outputs at the surface level are made for wind speed (WS10), wind direction (WD10) at 10 m above ground, temperature (T2), and relative humidity (RH2) at 2 m above ground. For upper air the outputs from WRF are compared at 925 hPa and 850 hPa levels for wind speed, wind direction, temperature and humidity respectively. The model results extracted from the nearest grid points to observation locations are used for comparisons. Visual comparisons are made for three coastal stations Slidell, Pascagoula, and Gulfport, and seven inland surface stations Maccomb, Jackson Thomson, Hattisburg, Pine, Natchez Hardy, Kessler and Hammond that fall in the model inner domain (Figure 2).

A number of model performance indicators for air quality and meteorological predictions are prescribed by several workers [10, 52–56]. The statistical metrics in the present analysis include Pearson correlation coefficient (r), Mean error (ME), Multiplicative bias (MB), Mean Absolute Error (MAE) and Root Mean Square Error (RMSE) as given below:

$$\begin{gathered}
r = \frac{\sum_{i=1}^{n}\left(f_i - \overline{f}\right)(o_i - \overline{o})}{\sqrt{\sum_{i=1}^{n}\left(f_i - \overline{f}\right)^2}\sqrt{\sum_{i=1}^{n}(o_i - \overline{o})^2}}, \\
\mathrm{ME} = \frac{1}{n}\sum_{i=1}^{n}(f_i - o_i) = \overline{f} - \overline{o}, \\
\mathrm{MBIAS} = \frac{\overline{f}}{\overline{o}}, \\
\mathrm{RMSE} = \sqrt{\frac{1}{n}\sum_{i=1}^{n}(f_i - o_i)^2}, \\
\mathrm{SD} = \sqrt{S_f^2 + S_o^2 - 2S_f S_o r_{fo}}, \\
\mathrm{MAE} = \frac{1}{n}\sum_{i=1}^{n}\left| f_i - o_i \right|,
\end{gathered} \tag{1}$$

where o_i is an observable variable, f_i is a predicted variable, overbar represents average over all the data, and "n" is the total number of locations that predicted data are compared against observations. Mean error is a measure of overall bias for continuous variable, multiplicative bias is the ratio of the means of the forecasts and the observations. r is the correlation between the forecasts and observations. SD is the standard deviation of the error (f-o), where S_f is the standard deviation in forecasts and S_o is the standard deviation in observations. Root Mean Square Error is the square root of the average squared error of the forecasts. Specifically, MAE is less influenced by large errors and also does not depend on the mean error. The RMSE can be subdivided in a systematic part and a random part, and only the systematic part is of relevance here [52].

3. Results and Discussion

The synoptic weather situation for the study period is analysed from the NCEP FNL analysis data at 18 CST 7 June 2006 (i.e., 00 UTC 8 June) (Figure 3) for the sea level pressure and winds. There are two low-pressure systems, that is, 1005 hPa over Atlantic Ocean near the east coast and 1008 hPa over the land region in the western US. Strong cyclonic winds ($\sim$20 $\mathrm{ms^{-1}}$) extending to large area are seen around these two low-pressure centers. Winds in the lower atmosphere (at 925 hPa) are strong northerly over the west coast and strong southwesterly over the east coast under the influence of the above low pressure centers. Westerly winds or northwesterly winds over the United States with high-pressure conditions over the western, northern parts, moderately high pressure conditions over the central and southeastern US and low pressure conditions over the southern parts of the US are seen. The winds in the southeastern US are northwesterly with strength of about 5 $\mathrm{ms^{-1}}$ in the states Louisiana, Mississippi, and Alabama. Thus the synoptic weather condition for the study period is influenced by the low pressures. Model results are analysed following the qualitative as well as quantitative evaluation procedures as illustrated in various works (namely, Mao et al. [7], Zhang et al. [8], Chandrasekar et al. [19], Gilliam et al. [20], Willmott [52], and Lyons et al. [53]). In the qualitative evaluation, visual comparisons are made for observed, simulated meteorological and air quality fields. In the quantitative evaluation, various statistical skill indices are estimated as a measure of model performance.

3.1. Sensitivity Analysis with PBL and Land Surface Physics. The critical meteorological components in the air quality assessment are the 2-d winds, PBL height and its spatial variation, vertical structure of winds, temperature, humidity in the PBL, time series of PBL height, and surface variables. The above components characterize the transport, PBL stability and diffusion, and their diurnal variations. The simulation of these fields and their sensitivity to different PBL-LSM options are discussed below.

3.1.1. Wind Field and PBL Structure. The transport of chemical species mainly depends on atmospheric flow fields at lower levels, and so the model-derived flow fields for the third domain are analyzed for experiments with different PBL and LSM options. Sea-land breeze is a chief mesoscale flow in the Mississippi Gulf Coast and is predominantly observed during the daytime in the summer synoptic condition. The simulations in all experiments revealed development of diurnally varying local flow pattern, that is, offshore wind during the morning conditions and onshore winds in the afternoon. The sea breeze phenomenon could be captured well by all the simulations. Wind field at the surface (10 m level) from the simulations with different physics options is shown in Figure 4 for afternoon condition corresponding to 13 CST 10 June 2006 when significant sea breeze development in the study region is noticed in the simulations. The flow pattern shows strong southerly/southeasterly winds associated with sea breeze and its considerable extent inland in the afternoon time. Slight differences are noticed in the direction and magnitude of simulated onshore and offshore winds across different experiments. The flow fields are approximately similar in the experiments (YSUSOIL, YSUNOAH, ACMSOIL, ACMPX), (MYJSOIL, MYJNOAH) and (YSURUC, ACMRUC, MYJRUC). The notable differences in the wind field are the southeasterly onshore winds becoming southerly and southwesterly on crossing the coast in Mississippi in the first group of experiments while becoming week southerly winds in the second group. The simulated onshore southeasterly winds are also stronger in the second group of experiments. While the flow field smoothly varies across the domain in both the YSU, ACM cases it shows a complex pattern in the MYJ cases. A convergence in the surface level flow is noticed along the Mississippi river (which runs along the geographical boundary of Louisiana and Mississippi) which is clearer in the experiments with RUC LSM (i.e., YSURUC, MYJRUC, ACMRUC). The surface heterogeneity, that is, land and water contrast along this major river and its direct influence on the flow pattern could be better represented with the RUC LSM. The RUC LSM seems to better resolve the surface processes for example the simulation of surface heat and moisture fluxes and thus the surface wind flow pattern using its high resolution (6 layer) soil model and coupled hydrology, vegetation models. The onshore flow at the Gulf Coast is mostly southerly in the experiments with YSU, ACM PBL while it is predominantly southeasterly in the experiments with MYJ PBL. Experiments with MYJ PBL tend to give slightly stronger winds (4–10 $\mathrm{ms^{-1}}$) and also more convergent flows. The progression of the sea breeze front is much inland in these cases. Thus MYJ PBL scheme has produced stronger winds than those with the non-local first-order schemes (YSU, ACM) during both onshore and offshore flow scenarios. The difference in the wind field simulation in the experiments may be due to the difference in the parameterization of eddy exchange coefficient which is based on TKE in MYJ and dependent on similarity formulations in YSU and ACM respectively. The complexity in the flow field is reduced in the simulations at 925 hPa and 850 hPa levels and not many differences in results are noticed among different experiments. Thus the

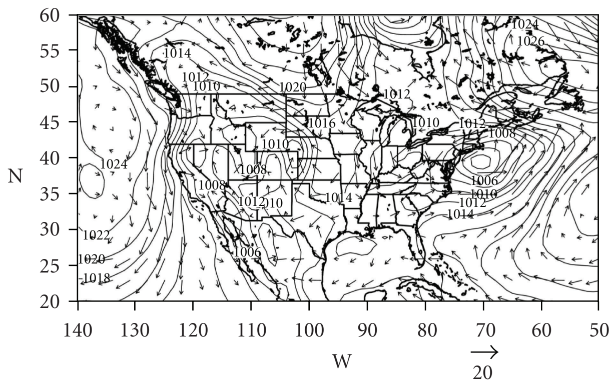

Figure 3: Sea level pressure (hPa) and wind flow in the lower atmosphere at 18 CST 7 June (00 UTC 8 June).

dynamics of the flow field could be better represented in the simulations with RUC LSM.

Comparisons are made with radiosonde observations at lower atmosphere to evaluate the model-simulated atmospheric structure and the errors in the key meteorological variables. Vertical distribution of potential temperature, relative humidity, wind speed, and wind direction in respect of different experiments along with upper air radiosonde observations is shown in Figure 5 for Slidell station in Louisiana adjacent to the coast. In general, vertical profiles of simulated quantities (except RH which is dependent on temperature) in all experiments are in good agreement with observations at 6 CST and 12 CST on 10th June 2006. The morning observation profiles (06 CST) indicate highly stable stratification in the layer 0 to 300 m AGL with inverse Obukhov length ($1/L$) values of the order 0.003. This surface stratification is not captured well by the model and all the experiments indicate an underestimation of temperature below 250 m. In the morning stable conditions, the profiles show increasing of potential temperature (inversion), decreasing humidity, and increasing or decreasing of wind speed coinciding with shifts in wind direction (wind shear) with height. The common finding from the literature is that the MYJ scheme generally outperforms YSU or ACM for the nighttime boundary layer. However in our experiments YSU, ACM PBL have produced more realistic profiles during stable conditions than other schemes. These schemes are formulated to be advantageous for the daytime conditions. However, they seem to perform better than other schemes during stable conditions also, as indicated in present results. In the daytime convective conditions (12 CST), observations indicate a steep unstable layer up to 300 m height and a well-mixed boundary layer development up to a height of 1800 m above the ground. RH profiles from MYJ PBL indicate errors up to 20%–25% overestimation within 2500 m height layer in daytime and within 500–1500 m layer in the nighttime. RH profiles given by YSUSOIL, YSUNOAH, ACMNOAH, and ACMRUC are found to give more realistic profiles in both stable and unstable conditions. Generally, higher RH is estimated in the runs MYJSOIL, MYJNOAH, MYJRUC and ACMNOAH. Model runs with YSU, ACM PBL schemes have better produced the temperature and humidity distributions, particularly the shallow unstable layer and the deep convective boundary layer characteristics as noticed in nearly constant model values vertically as in observations. There are significant differences in the wind speed up to 3 km simulated by different simulations. Model experiments YSUSOIL, YSURUC overestimated wind in the levels below 500 m, but compared well with observations above 500 m. The profiles simulated in ACMNOAH, ACMSOIL experiments agree well with observation profiles. The MYJSOIL, MYJNOAH, MYJRUC underestimate in the layer 1.5 km and overestimate in the layer 1.5 km–3 km. The profiles from YSUNOAH agree well up to 2000 m and show little underestimation in the layer from 2000 to 3000 m. Thus for wind speed the simulations ACMSOIL, ACMNOAH give better profiles and next to them YSUNOAH gives reasonable comparisons. In evening conditions (not shown) the profiles indicate development of a residual layer and experiments with YSU, ACM reproduced its characteristics in the lower 1-2 km region. Thus for the vertical atmospheric structure the MYJ scheme shows poor agreement with observations and the vertical tendency of the variables is better simulated by the YSU, ACM schemes. The LSMs seem to influence the humidity and wind distributions rather than temperature. The multilayer soil model simulates the soil temperature in different layers but it treats the soil moisture as a seasonal constant dependent on the land cover. The NOAH and RUC land surface models contain detailed equations for soil hydrology, evapotranspiration, and snow/ice processes and therefore they are supposed to produce the diurnally varying surface fluxes of heat and moisture more realistically than the simple soil model. The temperature, humidity and wind distributions in the lower atmosphere are directly influenced by the surface effects which are treated more comprehensively in the NOAH and RUC LSMs.

One of the crucial parameters that affect air quality is the atmospheric boundary layer height. The PBL height limits the effective mixing region in the lower atmosphere and characterizes the atmospheric diffusivity. The simulated daytime mixing height from different experiments with PBL and LSM options is shown in Figure 4 in grey shades corresponding to 13 CST 10 June 2006. The MYJ scheme defines the PBL height using TKE, while the YSU and ACM schemes derive it from the bulk Richardson number. The simulated nocturnal PBL height varied from 25 to 100 m at different locations. However, significant differences are noticed in the daytime boundary layer height produced by different experiments. The PBL development during the daytime is largely due to convective turbulence, which is simulated variously by the different PBL models. The spatial PBL height pattern is smoother in the experiments with YSU, ACM schemes which are based on eddy-diffusivity formulations. The pattern of boundary layer height across the domain in the experiments with MYJ scheme is more complex and indicates to be more of convective turbulence. The PBL height at the coast is about 200 m in all simulations. Over the land the PBL height varied as 1,200–2,400 m (YSUSOIL, YSURUC), 1,200–1,800 m (YSUNOAH), 900–1,800 m (MYJSOIL, MYJRUC), 900–1,200 m (MYJNOAH),

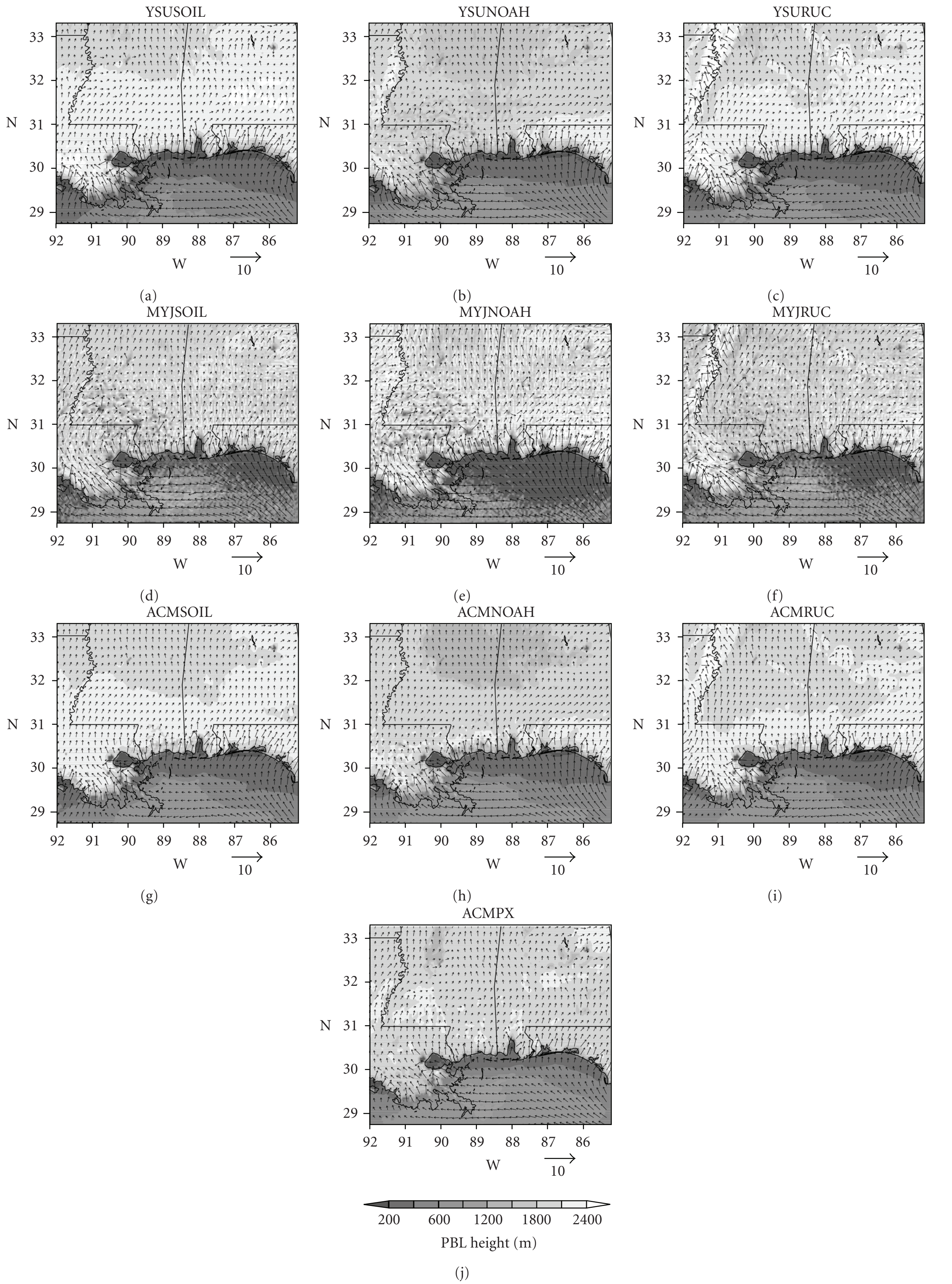

Figure 4: Low-level wind field (ms^{-1}) and PBL height (m) simulated in the model fine domain from experiments with different PBL and land surface physics options at 13 CST 10 June 2006.

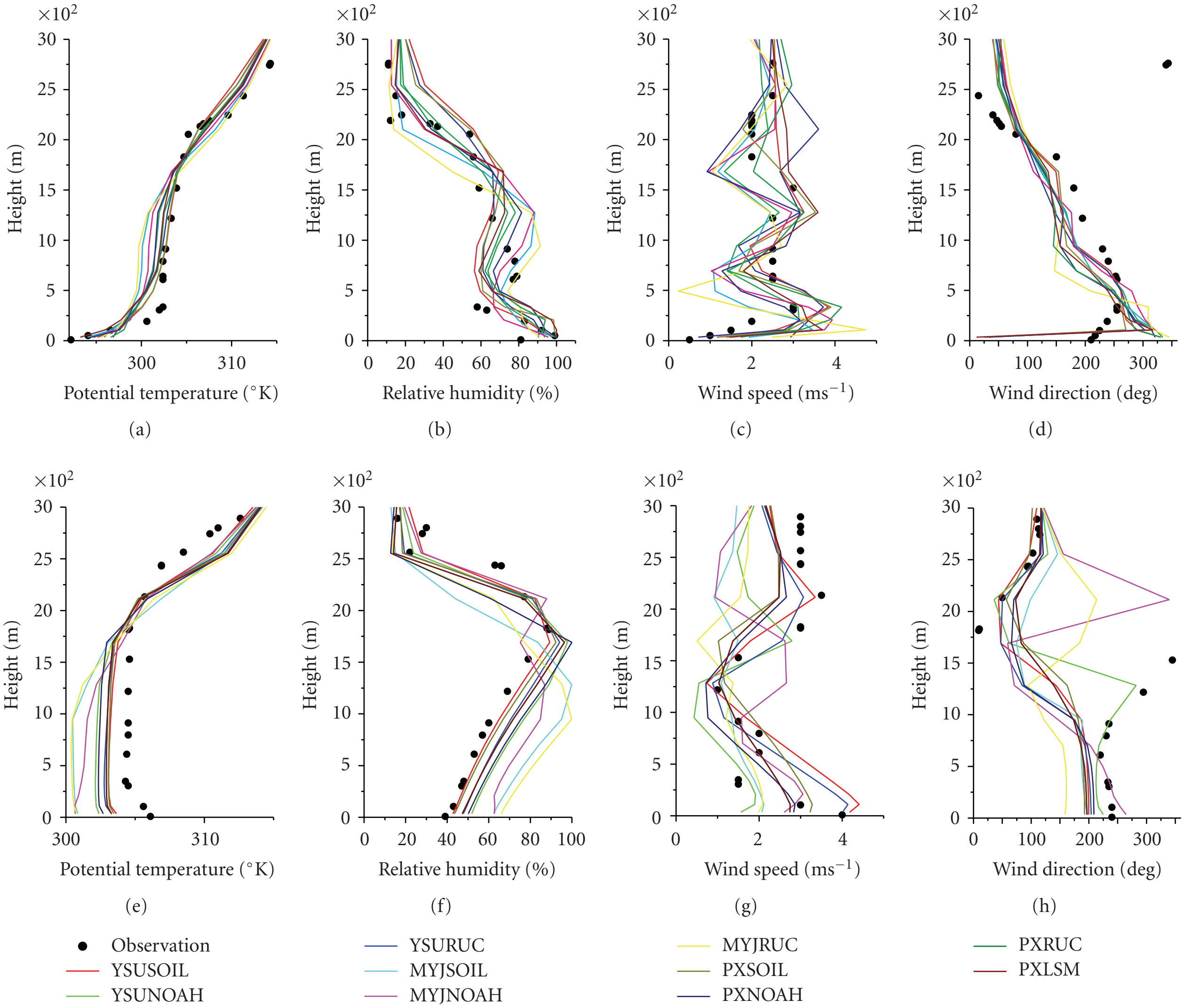

Figure 5: Vertical distributions of potential temperature, relative humidity, wind speed, and wind direction at Slidell station in Louisiana on 10th June, 2006. The top panels (a, b, c, and d) are for 06 CST and the bottom panels (e, f, g, and h) are for 12CST.

1,500–2,400 m (ACMSOIL, ACMRUC), 1,500–1,800 (ACMNOAH) and 1,800–2,100 (ACMPX). Thus, the YSU and ACM PBL schemes produce deeper boundary layer than the MYJ scheme and the spatial range of deeper PBL height is wider with YSU than the ACM. These results are consistent with the past findings [28, 32]. The 5-layer soil model tends to give higher PBL development when used with most PBL schemes probably because it has also predicted a slightly higher daytime temperature than the other schemes (discussed subsequently) thus causing relatively higher convective boundary layer growth.

The selected PBL schemes in the current study use different algorithms for the calculation of PBL height. The YSU, ACM schemes calculate the PBL height as a function of critical Richardson number from the vertical temperature, wind distribution while the MYJ scheme calculates it from the vertical turbulence kinetic energy distribution. As seen from the vertical potential temperature distribution (Figure 5(e)) the experiments with YSU, ACM produce deeper mixing layers than the MYJ scheme, as also found from past studies [25, 32]. The maximum PBL growth indicated from the profiles is about 1,800 m corresponding to the convective conditions at 12 CST on 10th June 2006. The PBL height indicated from the radiosonde profiles is about 200 m during the morning conditions and about 1800 m during the convective daytime conditions. The PBL height is estimated from available vertical soundings at Slidell, LA by using Richardson number (RiB) with a critical value of 0.25. However, the observed PBL height from radiosonde profiles has some error depending on the vertical resolution of the observations. The vertical resolution of the radiosonde observations is about 50 to 100 m in the region 0 to 500 m AGL and about 200 m in the region 500 m to 1500 m AGL. Hence errors of the order of 200 m could arise in the

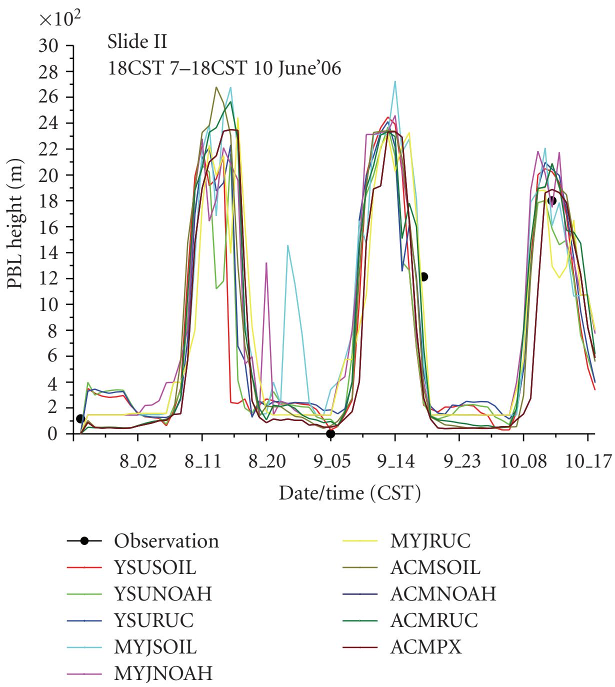

Figure 6: Time series of simulated PBL heights from experiments with different PBL, LSM options at Slidell. Black dots indicate estimated PBL heights from radiosonde observations.

estimated daytime PBL height and about 50 m to 100 m in the nighttime PBL. The model diurnal evolution of the PBL height values for different simulation cases along with estimated values are shown in Figure 6 for Slidell. From these plots it is seen that experiments with YSU and ACM PBL schemes exhibit relatively faster growth and decay of the daytime boundary layer height than those with TKE schemes as also found in past studies [32]. The observed PBL height is about 100 m on the first night and 50 m on the second night while the model values range between 50 and 350 m. This difference in the estimation and simulation is due to the coarse radiosonde observations used for estimation as discussed above. The nighttime PBL height is simulated with reasonable values (∼250 m) in most simulations except MYJNOAH and MYJSOIL which produced spikes of up to 1200 m during nighttime on the second day. Such deep boundary layer development is possible during daytime convective conditions alone and thus indicates unphysical behaviour from MYJNOAH and MYJSOIL during night conditions. For the daytime experiments with 5-layer soil diffusion and RUC LSM produced relatively deeper boundary layers than those with NOAH, PX LSMs. The YSU, scheme with NOAH LSM often produced shallow boundary layers during the diurnal cycle as also found in the work of Zhang et al. [32]. The estimated PBL height is available for mostly stable night conditions and the simulated mixing height from all experiments agrees with the estimates (Figure 6). Simulated PBL height in YSU, ACM cases closely agrees with the value derived from profile observations through RiB at 12 CST 10 June 2006. The present results indicate a general overestimation of stable boundary layer height in experiments with YSU and MYJ as found in earlier studies by Hanna and Yang [21] and Steeneveld et al. [22] while using similar schemes.

3.1.2. Diurnal Variations in Surface Meteorological Parameters. The parameters temperature, humidity, clouds and shortwave radiation influence the formation of ozone. Cloud effects would be generally important for the estimation of photolysis rate in the model. However as the simulation period is characterized with dry weather situation the model cloud effects are not considered important for the study. The time series of hourly outputs from simulations in the fine grid (4 km) domain are shown in Figures 7, 8, 9, and 10 for the air temperature (T2), relative humidity (RH2) at 2 m, wind speed (WS10) and wind direction (WD10) at 10 m above ground for model grids corresponding to a few observation sites (Hammond, Jackson, Gulfport, Hattiesburg, Evergreen, Kessler, Natchez Hardy, MacComb and Pascagoula). The stations Pascagoula, Gulfport, and Hammond are located along the coast and all other stations are located inland. The observations are shown in black lines or dots. Surface temperature is a crucial parameter as it drives the boundary layer and influences the mixing of pollutants. The accurate estimation of surface temperature ensures to some extent the structure of the boundary layer and its influence on the dispersion characteristics. A gap in observations exists between 20 CST 8 June to 20 CST 9 June at some locations. The model reproduced the diurnal temperature cycle and its mean at most locations. The model overestimated the minimum temperatures during nighttime (warm bias) except at the Pascagoula and slightly underestimated the maximum temperature during the daytime. The diurnal range of various parameters is higher for the inland stations than for the coastal stations. The daytime temperature is slightly underestimated in most of the simulations. Experiments YSUSOIL, ACMSOIL, ACMNOAH, and ACMRUC have consistently reproduced the magnitudes of the surface air temperature and their diurnal range at most locations and at most times while others led to significant errors at different times and locations. The YSUNOAH, YSURUC, MYJSOIL, MYJNOAH, MYJRUC indicate a warm bias in the nighttime temperature at many locations while ACMPX indicates cold bias in daytime temperature. In general simulations using SOIL model tend to estimate higher temperatures than those using other surface schemes. This higher temperature prediction with SOIL model is also seen to produce higher PBL growth from the corresponding runs as noted in earlier discussions. Unlike temperature, the diurnal evolution of relative humidity widely varied among the different experiments. The RH is generally overestimated during the simulation in all cases. In general, irrespective of the physics option used the magnitude of RH is better estimated for Hattiesburg, Pascagoula, Evergreen, and Kessler. The poor performance of the model for RH at some locations (namely, Natchez, and Jackson) may be due to the representation of vegetation and soil category data at those locations which needs to be examined. Most of the simulations show wet biases in the nighttime (cf.

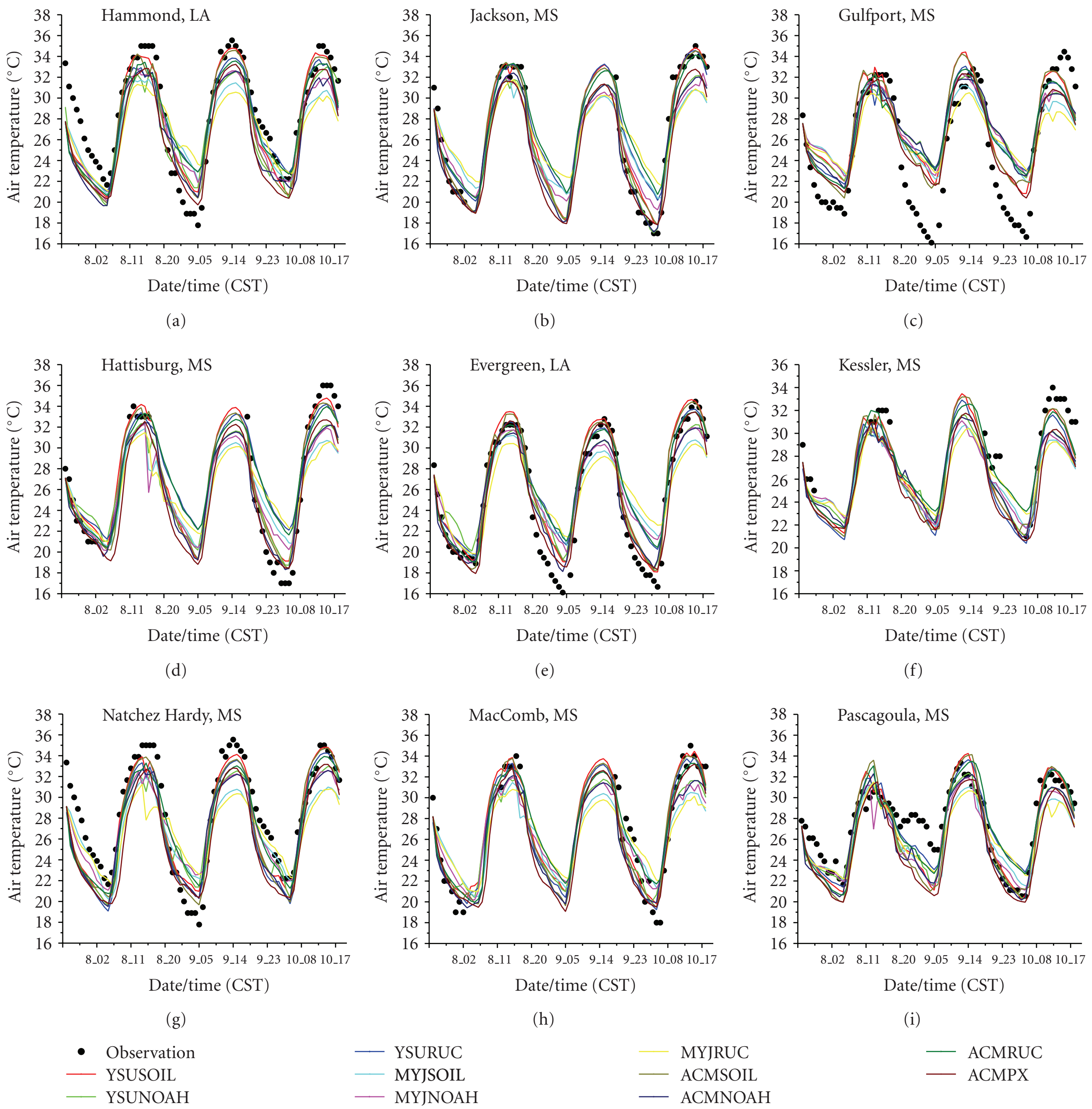

Figure 7: Time series of the observed and simulated surface air temperatures (at 2 m) during 18 CST 7–18 CST 10 June 2006 at 9 surface stations in the fine grid domain. The legend is the same for all panels.

00CST-05CST) and also wet biases in the daytime (cf. 11CST-20CST). Since the relative humidity is closely linked to the temperature, the underestimation of the daytime temperature may have caused the overestimation of the relative humidity. The largest humidity biases are found with MYJ PBL. The YSUSOIL and ACMPX give overestimations for most locations. The YSUSOIL, YSUNOAH, YSURUC, ACMNOAH, ACMRUC have given better diurnal values and range of RH at most locations in the study region. The use of NOAH, RUC land surface schemes did improve the RH prediction with YSU, ACM schemes but not appreciably with the MYJ scheme. It appears that fog occurs in the model very often at night with higher RH values of ~50% (wet bias). This unrealistic humidity in the model would lead to triggering of wet deposition and aqueous chemical processes in the model and may result in unrealistic chemical concentrations and depositions.

Time series of wind speed at 10 m height (Figure 9) shows that all the simulations indicate deviations in diurnal wind speed evolution. Wind is overestimated (cf. 20CST–05CST) by most experiments at MacComb, Hattiesberg, Jackson, Hammond, Natchez, and Kessler in the nighttime

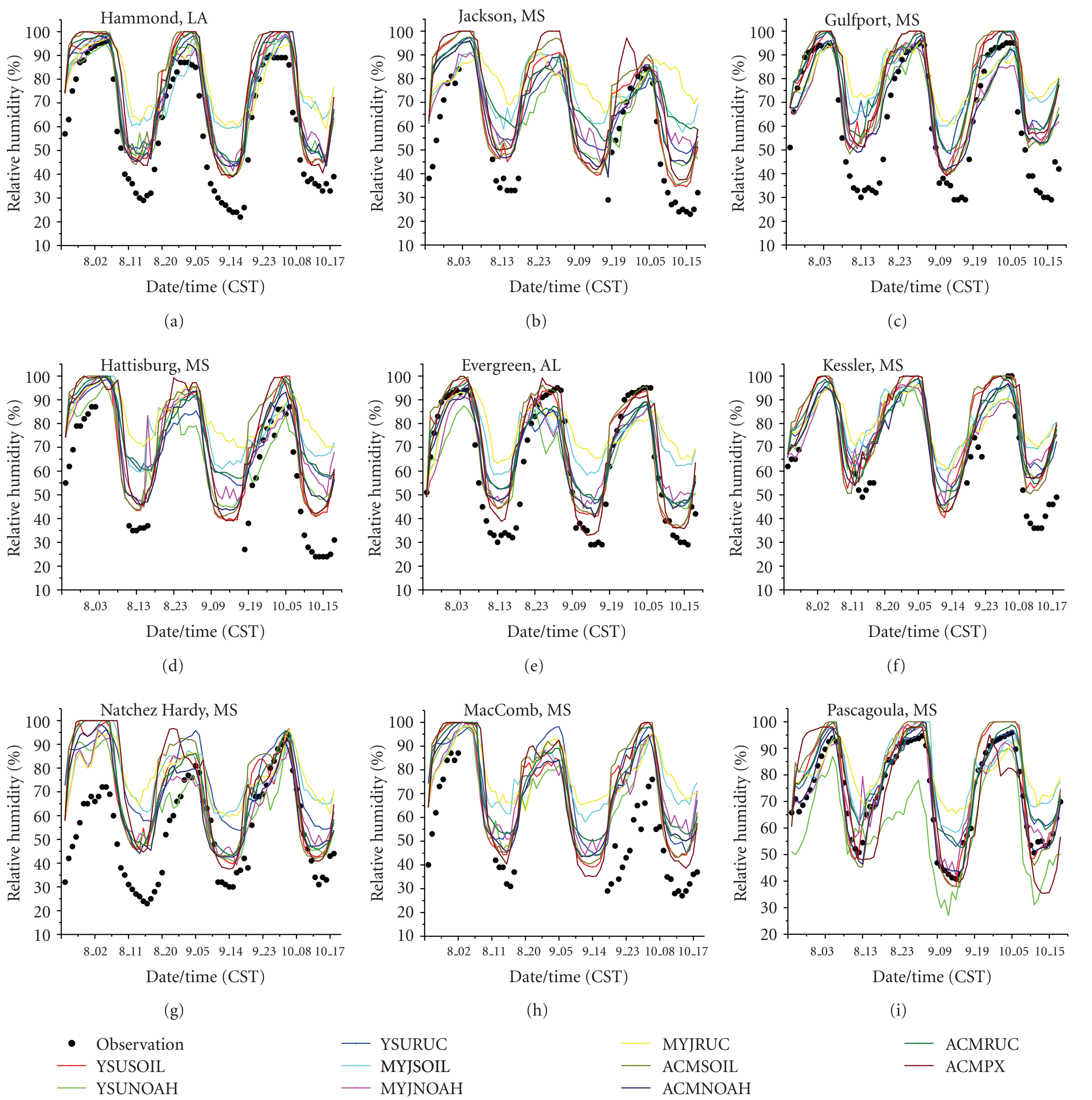

Figure 8: Time series of the observed and simulated surface relative humidity (at 2 m) during 18 CST 7–18 CST 10 June 2006 at 9 surface stations in the fine grid domain. The legend is the same for all panels.

(cf.20CST-05CST) and at Pascagoula in the daytime (cf. 13CST–20CST). Overestimation of wind speed during the night appears to be a quite common experience with WRF [28, 56, 57]. Large deviations in wind speed are noticed from experiments YSUSOIL, YSURUC, MYJSOIL, MYJNOAH and MYJRUC which overpredicted wind at many locations. Experiments YSUNOAH, ACMNOAH, and ACMPX tend to provide better estimations of wind speed and its diurnal range at most locations. In the plots of diurnal wind direction (Figure 10) observations are indicated in solid black line and the values from different experiments are shown in color symbols. The differences in the simulation of wind speed in different PBL cases are probably due to the variation in parameterization of eddy exchange coefficient which is based on TKE closure in MYJ and on friction velocity and PBL height in YSU and ACM, respectively. Experiments with YSUNOAH, YSURUC, ACMRUC, and ACMPX tend to produce the nearest comparisons. For 10 m wind direction, the model reproduces well the diurnal cycle at most locations. In all the experiments the wind direction is reasonably well simulated for the stations Pascagoula, Kessler, Natchez, Maccomb Gulfport locations. Some deviations are found in the case of Hattiesburg, Evergreen, and Mobile which may be due to the inadequate representation of terrain in the model. The maximum differences in wind direction are about 50 degrees (Figures 5 and 10) in the cases with MYJ PBL, which is found to produce large discrepancies at many locations. These discrepancies in wind directions corroborate with earlier results from Hanna and Yang [21], while using TKE-based PBL parameterizations. Overall, the experiments YSUNOAH, ACMPX simulate the wind direction better than the others.

3.1.3. Statistical Evaluations for Sensitivity Runs. Results from statistical analysis for various meteorological parameters are discussed here. The statistical analysis is made between observations and model outputs for temperature, relative humidity, wind speed and wind direction at surface and a few levels in the lower atmosphere (925 hPa and 850 hPa). The statistics is computed for each station and at all observation hours for each simulation case as per the procedure outlined in Section 2.6. The aggregate of this analysis is presented here. The sensitivity of WRF to various PBL/LSM schemes is quantified by using five basic statistical measures namely, the Pearson correlation coefficient (R), mean error (ME), multiplicative bias (BIAS), mean absolute error (MAE), and the root mean square error (RMSE) and are shown for the surface level in Table 2. These statistical indices are selected as they are relatively simple to compute and for interpretation. The aggregate statistics is provided in Table 2 for temperature, humidity, wind speed and wind direction, respectively, for the surface meteorological variables. The statistics is noted to improve with altitude for various parameters. For 2-m air temperature, the model runs YSUSOIL, YSUNOAH, YSURUC, MYJSOIL, MYJNOAH, and ACMPX gave relatively higher correlations (0.41–0.45), and lower ME (0.02–0.50°C), lower MAE (1.87–2.3°C), lower RMSE (2.38–2.61°C) than the other runs. The model runs ACMRUC, MYJRUC, ACMNOAH, and ACMSOIL indicate improvement in statistics at 925 hPa, 850 hPa levels over the values at surface level where the above runs show poor correlations, large ME and MAE. The statistical results for ACMNOAH are better at 925 hPa and for ACMPX at 850 hPa, respectively. The YSU PBL scheme is noted to produce consistent results at all levels with good correlations and relatively lower error metrics. The YSU scheme with 5-layer soil model has given relatively better statistics than the NOAH LSM for 2-m air temperature while also producing best statistics at 925 hPa and 850 hPa levels.

The statistical skill scores for humidity are relatively poor than for temperature in all the sensitivity runs. For RH model runs YSUSOIL, YSUNOAH, MYJNOAH, ACMNOAH, and MYJRUC yielded higher correlations (0.2–0.27), lower values of ME (5.2%–8.8%), BIAS (1.1%–1.22%), MAE (10.38%–12.8%) and RMSE (12.8% to 15.2%), respectively. The statistical results are better for ACMNOAH at 2 m, 925 hPa, for ACMRUC at 925 hPa, 850 hPa levels, for ACMSOIL at 925 hPa, for ACMPX at 2 m, 850 hPa and for MYJSOIL at 850 hPa, respectively. The model runs MYJSOIL, ACMSOIL, YSURUC and ACMRUC have produced poor statistics for RH at 2 m. The YSUSOIL, YSUNOAH have consistently given better statistics at all three levels 2 m, 925 hPa, 850 hPa. Of these two combinations the YSUSOIL gives the best statistics for RH prediction as seen from the relative values of R, ME, BIAS, MAE and RMSE, respectively. Of the multilayer soil and NOAH LSMs the latter is supposed to simulate the diurnal RH better as it includes explicit soil hydrology and vegetation processes. However, for the present dry weather case the soil hydrological effects may not have contributed much to the RH simulation. The relative performance of NOAH and soil models needs to be studied further considering a wet weather condition.

For wind speed at 10 m the model runs YSUSOIL, MYJSOIL, YSUNOAH, MYJNOAH, ACMPX yielded better statistics, that is, higher correlations (0.25–0.27), lower values of ME (0.05–0.7 ms^{-1}), BIAS (1.2–1.4 ms^{-1}), RMSE (1.5–1.7 ms^{-1}) (Table 2). The present RMSE values are lower than the values reported by Hanna and Yang [21], for wind speed. The statistics for MYJRUC are better at 925hPa, 850 hPa, for MYJSOIL at 10 m, 850 hPa, ACMRUC at 925 hPa, 850 hPa levels and for ACMPX at 10 m, 850 hPa levels. The YSUSOIL and YSUNOAH have consistently given better statistics at all three levels 10 m, 925 hPa and 850 hPa. Of these two the YSUNOAH yielded the best statistics for wind speed at all three levels with the lowest values of ME, BIAS and RMSE, respectively.

Statistical evaluation of wind direction is complicated as large errors are likely to arise whenever wind fluctuations occur around 0°/360° in model and observation values. Hence in the present study the u-wind, v-wind components from model and observations are compared. The mean of the statistics for the u, v wind components is taken as a measure of model performance for wind direction. For u, v winds at 10 m the model runs MYJSOIL, YSUNOAH, MYJRUC, ACMPX yielded better statistics with correlations (0.36–0.45), ME (0.1–0.47 ms^{-1}), BIAS (0.27–0.78 ms^{-1}), MAE (1.7–2.2 ms^{-1}) and RMSE (1.96–2.57 ms^{-1}), respectively. All these combinations have given consistent results for u, v wind components at 925 hPa and 850 hPa as well. However, the relative statistics indicates that the ACMPX produces the highest correlations and lowest values for ME, BIAS, MAE, and RMSE, thus provides the best statistics for wind direction at all levels followed by YSUNOAH. Thus, the aggregate of all statistics shows the best results are provided by YSUSOIL for temperature and humidity, YSUNOAH for wind speed and ACMPX, YSUNOAH for wind direction considering their performance within the boundary layer of the atmosphere.

3.1.4. Simulated Air Quality. Two gaseous chemical species O_3, NO_2 are considered to determine the sensitivity of air quality simulations to the meteorological fields generated from model runs with PBL, LSM parameterizations. The simulation period falls in late spring within two weeks of Summer Solstice. With weak synoptic-scale influence and near-solstice insolation, the primary effects will be essentially diurnal in terms of higher daytime ozone and localization of ozone under the influence of the local scale circulations in the study domain. Ozone is a secondary pollutant formed

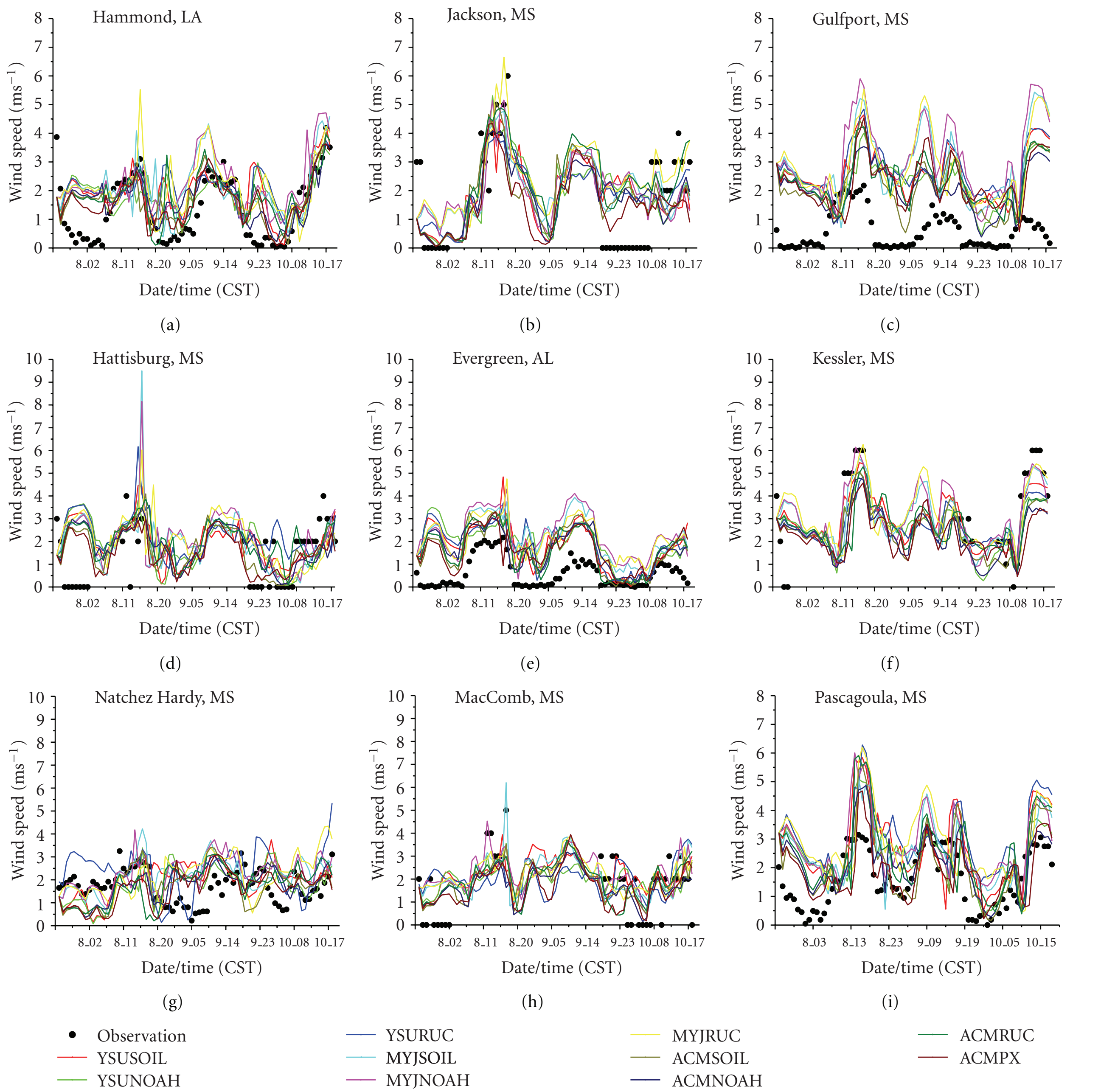

Figure 9: Time series of the observed and simulated wind speed (at 10 m) during 18 CST 7–18 CST 10 June 2006 at 9 surface stations in the fine grid domain. The legend is the same for all the panels.

in the lower atmosphere by a series of reactions involving the ultraviolet radiation and precursor emissions of nitrogen oxides (which are emitted from anthropogenic sources) and volatile organic compounds. The ozone formation in the troposphere is affected by local weather conditions such as winds, temperature, solar radiation, and horizontal and vertical diffusion characteristics which influence the precursor concentrations, reaction rates, formation, transport, and deposition. Ozone in the atmosphere has a dynamic equilibrium with NOx, which depends on the ambient temperature. Higher temperatures would lead to higher reaction rates and higher ozone production.

The spatial distribution of simulated ozone concentration in model runs with different PBL and LSM options for daytime condition corresponding to (10CST) 9 June 2006 is shown in Figure 11. The patterns of ozone formation are nearly similar for the YSU, MYJ PBL formulations. Slight differences in spatial patterns are found in these PBL cases according to the land surface physics used. The peak ozone concentration at this time is about 45–55 ppbv and

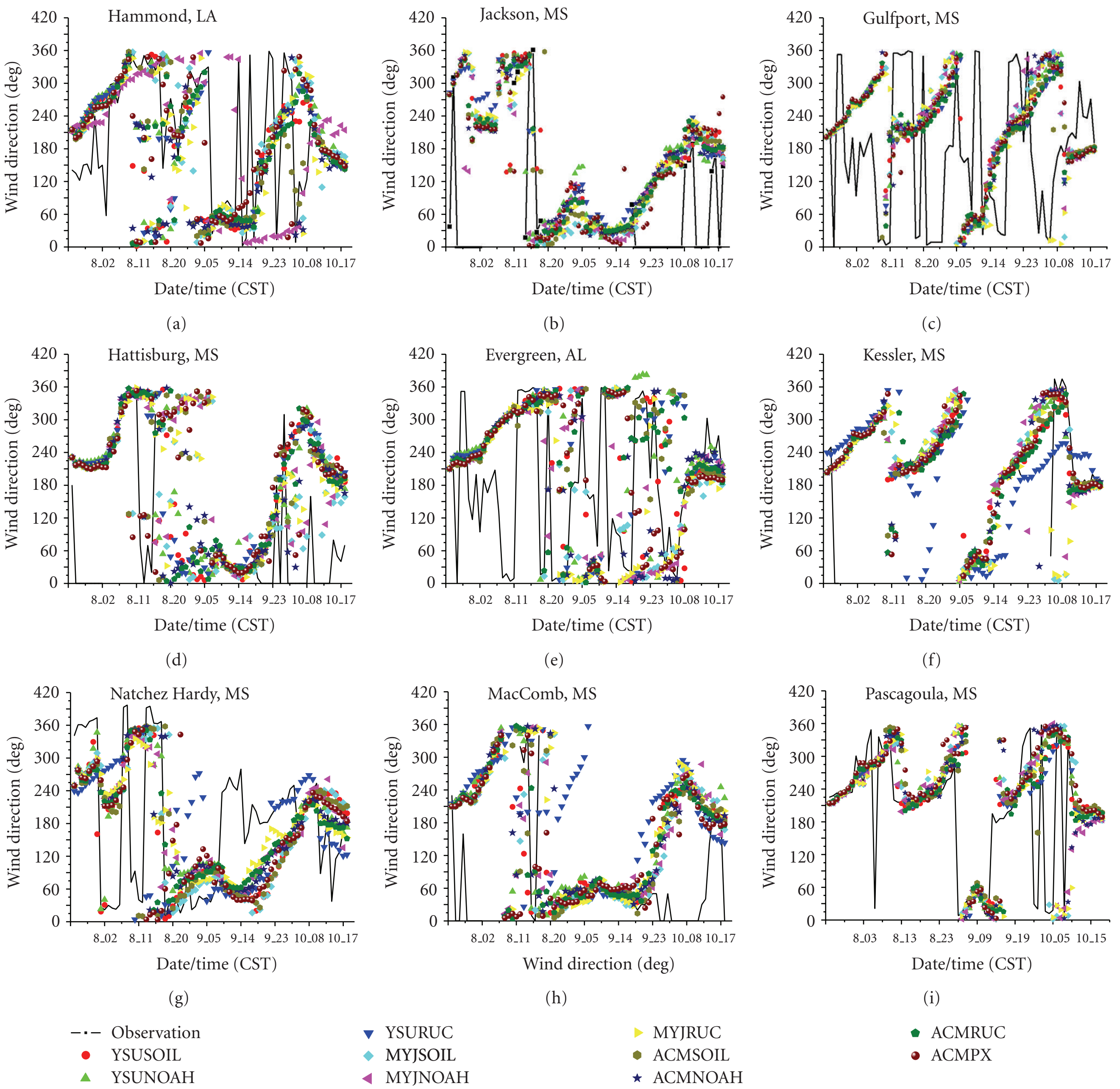

Figure 10: Time series of the simulated and observed wind direction (at 10 m) during 18 CST 7–18 CST 10 June 2006 at 9 surface stations in the fine grid domain. The legend is the same for all the panels.

is spread in southeast Louisiana and southern Mississippi in YSUSOIL, MYJSOIL cases, in the western parts of the domain in the YSUNOAH, MYJNOAH cases, and in central Mississippi region for YSURUC, MYJRUC cases, respectively. The differences in the results of the O_3 concentrations in different experiments are because of the variations in the simulations of atmospheric temperature, mixing depth, wind speed which affect the mixing and transport of pollutants. From the earlier discussions it is noted that the MYJ PBL gives relatively shallow mixing layers while the YSU and ACM provide moderately deep mixed layer development. The 5-layer soil model tended to develop relatively deeper mixed layers than in the cases using NOAH LSM. The model behaviour for ACM is clearly different from other PBL schemes for the simulated ozone pattern. The ozone simulated with ACM PBL seems to be more localized with higher concentrations in the northern Mississippi, eastern Louisiana and west Florida coast. Relatively very low concentrations are found in the oceanic region and in the southern parts of Mississippi, Louisiana and Alabama states. The peak ozone concentration in the runs with ACM PBL (≥65 ppbv) has formed along the northern part of Mississippi river and west Florida coast located to the south of Alabama. The convergence in the surface flow along the coast and along

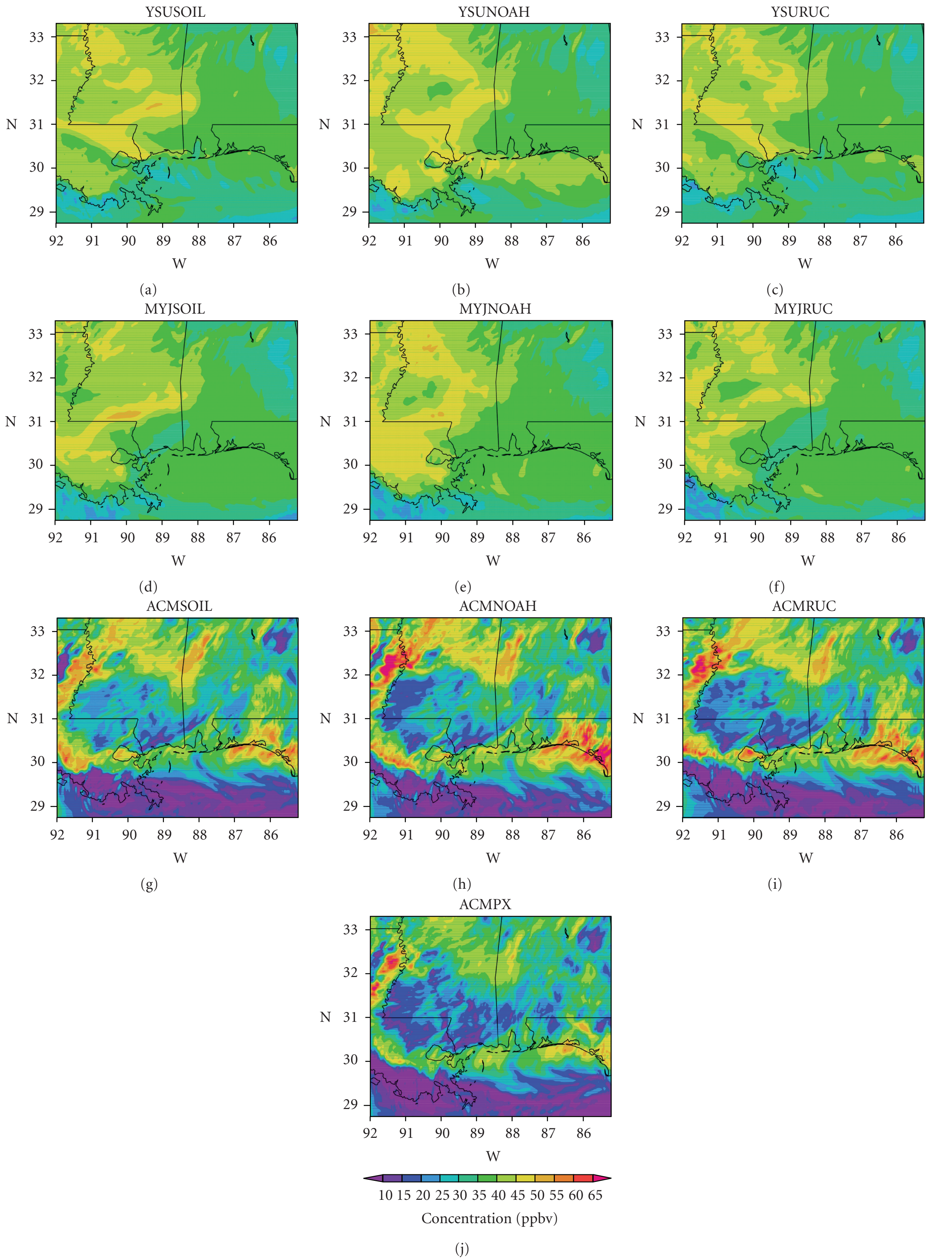

(a) (b) (c) (d) (e) (f) (g) (h) (i) (j)

FIGURE 11: Simulated ozone concentration (ppbv) in the model fine domain at the lowest level (30 m) from experiments with different PBL and LSM options at 10 CST 9 June 2006. The legend is the same for all panels.

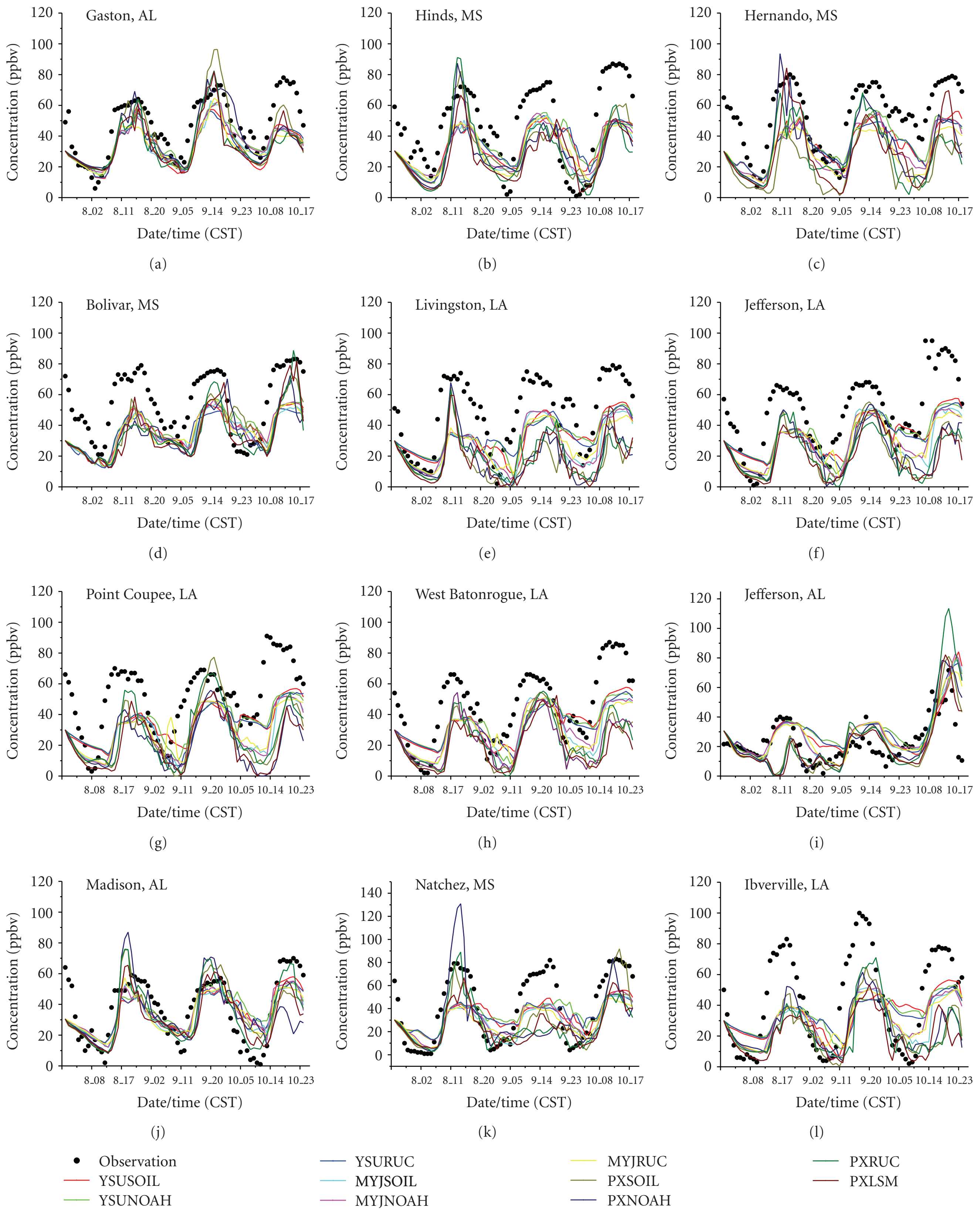

FIGURE 12: Time series of the simulated ozone concentration (ppbv) along with measured concentrations at a few air quality monitoring sites in the model fine grid domain at the lowest level (30 m) during 18 CST 7–18 CST 10 June 2006. The legend is the same for all panels.

Table 2: Statistical results for air temperature for experiments with different PBL and LSM physics for temperature, rh at 2 m and wind speed, u, v components at 10 m level.

Parameter	Experiment	R	ME	MBIAS	MAE	RMSE
Temperature (°C)	YSUSOIL	0.45	0.51	1.00	1.88	2.38
	MYJSOIL	0.43	−0.38	1.00	2.29	2.71
	ACMSOIL	0.31	0.77	1.00	3.26	3.78
	YSUNOAH	0.46	0.22	1.00	2.04	2.55
	MYJNOAH	0.42	0.02	1.00	2.10	2.58
	ACMNOAH	0.40	0.29	1.00	2.00	2.50
	YSURUC	0.46	0.98	1.00	2.09	2.62
	MYJRUC	0.39	0.02	1.00	2.43	2.92
	ACMRUC	0.39	0.97	1.04	2.34	2.73
	ACMPX	0.42	−0.71	1.00	1.94	2.42
RH (%)	YSUSOIL	0.27	7.92	1.22	10.66	12.89
	MYJSOIL	0.19	15.52	1.30	17.89	20.04
	ACMSOIL	0.14	6.99	1.15	16.04	18.68
	YSUNOAH	0.25	5.26	1.11	11.41	13.80
	MYJNOAH	0.23	8.84	1.17	12.77	15.18
	ACMNOAH	0.25	5.41	1.10	10.39	12.80
	YSURUC	0.19	7.69	1.15	12.32	14.71
	MYJRUC	0.23	8.84	1.17	12.77	15.18
	ACMRUC	0.15	7.98	1.15	12.11	14.63
	ACMPX	0.21	11.39	1.19	13.55	16.21
Wind Speed (ms^{-1})	YSUSOIL	0.27	0.40	1.63	1.32	1.64
	MYJSOIL	0.26	0.58	1.79	1.41	1.68
	ACMSOIL	0.20	0.19	1.67	1.40	1.73
	YSUNOAH	0.26	0.34	1.57	1.33	1.66
	MYJNOAH	0.26	0.70	1.86	1.41	1.74
	ACMNOAH	0.25	0.21	1.47	1.28	1.61
	YSURUC	0.25	0.62	1.91	1.45	1.79
	MYJRUC	0.24	0.83	2.00	1.49	1.83
	ACMRUC	0.25	0.42	1.61	1.36	1.70
	ACMPX	0.27	0.05	1.31	1.22	1.52
u, v wind (ms^{-1})	YSUSOIL	0.31	−0.33	2.40	2.26	2.58
	MYJSOIL	0.45	0.33	0.62	1.96	2.34
	ACMSOIL	0.21	0.10	0.38	2.11	2.47
	YSUNOAH	0.36	0.47	0.27	2.00	2.31
	MYJNOAH	0.31	0.48	0.71	2.05	2.40
	ACMNOAH	0.35	0.34	1.17	2.12	2.43
	YSURUC	0.35	0.45	1.23	2.15	2.52
	MYJRUC	0.41	0.20	0.78	2.20	2.57
	ACMRUC	0.37	0.86	0.93	2.08	2.55
	ACMPX	0.43	0.10	0.97	1.70	1.96

Mississippi river especially in runs with ACM PBL, RUC LSM caused the high ozone formation in these areas. Secondly the ozone distribution seems to be highly resolved spatially in the model runs with ACM PBL irrespective of the surface parameterization. The difference in the model behaviour for ozone with ACM is probably related to the differences in simulated vertical profiles of winds, temperature and the time series of various meteorological quantities which in turn are due to the variations in the model formulations for fluxes and eddy diffusivity relationships as discussed in Section 2.4. Overall the runs with NOAH LSM lead to the highest ozone amounts and MYJNOAH has larger area under high ozone concentration. The concentration pattern for NO_2 and SO_2 species indicates large plume-like peaks from sources in the northern parts of Mississippi, Alabama (not shown). The chief sources for these criteria primary gaseous pollutants are the coal fired power plants, manufacturing and other fuel combustion units distributed in the northern, central parts

Table 3: Statistical results for selected air quality species (O_3, NO_2) for experiments with different PBL and LSM physics.

Parameter	Experiment	SD	R	BIAS	RMSE
O_3 (ppbv)	YSUSOIL	10.69	0.68	−8.99	21.78
	MYJSOIL	11.45	0.68	−11.23	22.80
	ACMSOIL	12.65	0.59	−16.01	26.42
	YSUNOAH	10.30	0.66	−8.15	21.72
	MYJNOAH	11.41	0.71	−10.04	21.95
	ACMNOAH	12.67	0.54	−13.69	25.87
	YSURUC	9.64	0.66	−8.79	22.10
	MYJRUC	11.24	0.68	−10.74	22.46
	ACMRUC	13.58	0.60	−14.23	25.39
	ACMPX	11.70	0.56	−16.02	26.89
NO_2 (ppbv)	YSUSOIL	2.26	0.36	−4.48	6.18
	MYJSOIL	3.46	0.40	−3.19	5.73
	ACMSOIL	4.36	0.28	−1.79	6.73
	YSUNOAH	2.45	0.43	−4.34	6.02
	MYJNOAH	3.46	0.47	−3.19	5.64
	ACMNOAH	4.19	0.32	−1.78	6.38
	YSURUC	1.78	0.41	−4.57	6.18
	MYJRUC	3.30	0.32	−3.36	5.91
	ACMRUC	3.54	0.24	−1.94	6.39
	ACMPX	4.21	0.24	−1.53	6.81

and along the Gulf coast in the domain. As in the case of surface ozone, higher concentrations are found for NO_2, SO_2 for the model cases ACM and MYJ (not shown). The highest concentrations are provided by ACMNOAH while the largest spread of plume (dispersion) is given by YSUNOAH and MYJNOAH.

The diurnal evolution of ozone during 18 CST 7 June–18 CST 10 June 2006 (00 UTC 8 June–00 UTC 11 June 2006) from various sensitivity experiments with PBL, LSM options along with observations is shown in Figure 12 for ten monitoring stations (Natchez, Hinds, Hernando, Bolivar in Mississippi, Livingston, Jefferson, Point Coupee, West Baton Rogue and Iberville in Louisiana and Madison, Jefferson in Alabama). The simulated and observed ozone concentrations at many sites indicated 3 peaks corresponding to daytime production and 3 troughs corresponding to nighttime consumption. The peaks in diurnal ozone concentration occurred at 15 CST and the minimum at 04 CST, respectively, at most sites. Though the diurnal variations are simulated well, the WRF/Chem underestimated ozone mixing ratios at most locations. The predicted daytime ozone is about 10–30 ppbv less than the observed ozone at different locations in the study region. Underestimation of air temperature, overestimation of relative humidity and relatively stronger winds in the model might have contributed to the bias and inadequately capturing the peaks of ozone. The stronger winds would cause stronger advection of precursor pollutants and their less residence time affecting the photochemical processes in the atmosphere. The diurnal NO_2 is also underestimated at many locations (not shown). An important aspect of air quality forecasting is applied source strength which is defined in the present study in the model from the EPA emission inventory. As of now WRF/Chem does not incorporate an emission processing module like the SMOKE (Sparse Matrix Operator Kernel Emissions) developed for air quality models such as CMAQ (Community Multiscale Air Quality modeling system) and the emission data in WRF/Chem is interpolated directly from the EPA emission inventory. In the present study the emission data in WRF/Chem is interpolated from NEI2005 available at 4 km. The underestimation of NO_2 in the present study is an indication that the emission inputs obtained by interpolating the 4 km NEI 2005 data may not represent the reality accurately which may have caused the underprediction of O_3 peak. Some emission sensitivity tests in the model may need to be conducted using the other available inventory such as NEI1999, NEI2002, and NEI2008 (http://www.epa.gov/ttn/chief/eiinformation.html) to study the quality of the data and address this issue further. Secondly the 4 km NEI data may not be adequate while interpolating to model grids at the same horizontal resolution to represent the emissions variations at 4 km resolution. This approach followed in the current study might have led to underrepresentation of the source strength in the model grids thereby leading to underestimation of concentrations. Hence certain sensitivity tests with respect to the emission data resolution would also be needed to study its impact on the model performance. These emission sensitivity tests would help to identify whether current drawbacks in the modeling are due to WRF or simply due to inaccuracies in the emission database.

Model runs with different PBL and LSM options have shown large variation in the predicted ozone concentration. The nighttime ozone levels are slightly overestimated in the model runs with YSU PBL and slightly underestimated in the runs with MYJ and ACM PBL schemes. The daytime ozone is underestimated in the runs with all the PBL schemes and is captured relatively better in the runs YSUSOIL, YSUNOAH, YSURUC, ACMRUC and ACMNOAH. The diurnal range in ozone concentration is better estimated by the YSUPBL in association with either 5-layer or NOAH land surface schemes, which is probably because it also simulated the PBL height, wind speed, temperature, and humidity relatively better than the other options.

The statistical results for ozone and one of its precursor pollutants (NO_2) are given in Table 3 for model runs with various PBL and LSM physics. The statistical indices considered for the chemical species are correlation coefficient (R), mean bias (BIAS), standard deviation (SD); and root mean square error (RMSE), respectively. The model runs YSUSOIL, MYJSOIL, YSUNOAH, MYJNOAH, YSURUC, and MYJRUC yielded higher correlations (0.657–0.7), lower bias (−8.1–10.0 ppbv) and lower RMSE (2.78–22.46 ppbv). Though all the three land surface models with YSU PBL scheme have given reasonable statistics, the NOAH LSM has given the lowest bias as well as the lowest RMSE while also giving good correlation (0.658) among different model experiments. For NO_2 model runs YSUNOAH, ACMNOAH, MYJSOIL, MYJRUC, and ACMPX produced reasonably good statistics. Once again, the YSUNOAH yielded the least bias, lower RMSE and highest correlation. Thus considering all the three statistical measures the YSU PBL along with NOAH land surface model provides best combination for both meteorological and air quality fields for the summer episode in MS Gulf coastal region in the present work. The YSU PBL scheme with NOAH LSM is noted to be influential for the estimation of winds, temperature, humidity and mixing height. Overall, considering the qualitative as well as quantitative evaluations the WRF/Chem model with YSU PBL and NOAH land surface model provided best simulations for meteorological fields and air quality species O_3, NO_2 in MS Gulf coastal region. Though the mean concentration and the timing of the diurnal ozone is simulated well, its range is not captured in the study domain. The underestimation of temperatures and overestimation of winds in the simulation would have led to this underestimation of ozone by slowing down the generation and accelerating the advection process.

4. Conclusions

The study presents results from nested domain WRF/Chem simulations over the Mississippi Gulf coastal region with a grid resolution of 4 km for a 3-day moderately severe ozone episode in 8–11 June 2006. The simulations are conducted with an objective to evaluate the sensitivity of the air quality simulations to model meteorological fields in the online chemistry version. A total of ten sensitivity runs are performed with different PBL and land surface physics schemes to examine the model performance and to find an optimal setup of physical process schemes suitable to air quality study. The study covered three conceptually different PBL (YSU, MYJ, and ACM) schemes and four surface schemes (5-layer, NOAH, RUC, and PleimXue) available in the WRF3.1. Among the PBL options chosen both ACM and YSU PBL use the same first-order turbulence closure and both consider nonlocal mixing while the MYJ scheme uses a higher-order TKE closure. Of the various surface schemes employed, the NOAH LSM, RUC, PX are relatively more complex schemes than the simple soil model. The model meteorological results are evaluated at three levels (surface, 925 hPa, and 850 hPa) against observations in the innermost domain following standard procedures applicable to air quality modeling purposes. Qualitative and quantitative analysis is performed with extensive meteorological and air quality monitoring data. The model PBL heights are compared with radiosonde observations and using estimates arrived at through Bulk Richardson number. The model tends to overestimate the winds and relative humidity during both daytime and nighttime, and underestimate surface temperature during daytime.

Although there are mixed results for meteorological parameters many differences are noted from simulations using different combinations of PBL and LSM options. Among the tested PBL and land surface physics a few combinations give reasonably good predictions for various parameters of interest. The model runs with (MYJ PBL, 5-layer soil model) and (MYJ PBL, RUC LSM) give cold bias in daytime temperature and warm bias in nighttime temperature, while the ACMSOIL, and ACMPX give cold bias in daytime temperature. Qualitative and quantitative results reveal that for air temperature the model runs YSUSOIL, YSUNOAH, YSURUC, MYJNOAH, and ACMPX provide good results and that the YSU PBL with 5-layer soil thermal diffusion scheme produces best statistics. For RH, the model runs YSUSOIL, YSUNOAH, MYJNOAH, ACMNOAH, and MYJRUC provide reasonably good comparisons with observations and statistical results. YSUSOIL gives the best statistics for RH prediction with relatively lower values for ME, BIAS, MAE, MSE and RMSE. For wind speed the simulations ACMPX, YSUNOAH, and YSUSOIL have given better comparisons with observations. The YSUNOAH has given the best statistics for wind speed at all levels. For wind direction model runs ACMPX, YSUNOAH, and MYJSOL produce higher correlations and lower values for ME, BIAS, MAE, MSE, and RMSE at different levels. The YSU and ACM PBL schemes are found to give better simulations for mixed layer height. The 5-layer soil diffusion model and RUC LSM produced deeper boundary layers than with NOAH, PX LSMs. The YSUNOAH simulated PBL height closely matches with estimated values from radiosonde profiles. The differences in simulated meteorological quantities are because of the differences in parameterization of turbulent exchange coefficients in the three PBL schemes and the differences in land surface processes schemes. Thus for most meteorological parameters the YSU PBL scheme along with NOAH land surface model provides best results for the study in the MS Gulf Coast region. These findings corroborate the results from earlier studies [25, 26].

The patterns of simulated ozone, Nitrogen Dioxide concentrations from model runs with various PBL and land surface physics are noted to vary according to the variation in the simulated mixing depth and wind fields. The patterns of ozone concentration from model runs with ACM PBL are drastically different to those from YSU and MYJ schemes and reveal localization of simulated Ozone. Examination of the diurnal cycle and statistical analysis for most monitoring stations indicates that the run with YSU PBL and NOAH land surface model gives best results for all the chemical species with least BIAS, RMSE and highest correlation values. The diurnal range in ozone concentration is better estimated by the YSUPBL in association with either 5-layer or NOAH land surface schemes which is probably because it also simulated the PBL height, wind speed, temperature and humidity relatively better than the other options. Overall, the YSU PBL and NOAH land surface model provided best simulations for meteorological and air quality fields in MS Gulf coastal region. The present analysis conducted using the limited available boundary observations brings out certain important differences in model simulations while using typical PBL schemes having different formulations. To evaluate the model formulations more objectively a deeper analysis needs to be performed in terms of representation of the length scale, velocity scale of PBL and entrainment at the boundary layer, and so forth. To attempt such analysis special field experimental campaigns are planned in the study domain at different locations to generate high-resolution vertical PBL profiles, flux measurements and turbulence components using fast-sensor instruments.

The model has underestimated the daytime ozone which is probably due to the underestimation of temperatures and overestimation of winds. The underestimation of precursor pollutants also could be a reason for not adequately capturing the day time O_3 peaks. The emission inputs in the model need to be examined with sensitivity tests with different available datasets to address this issue further. Results from quantitative analysis indicate that the model has yielded correlations of about 0.46 for meteorological variables and about 0.66 for chemical species and thus shows good potential for air quality prediction in the Mississippi Gulf coast.

Acknowledgments

The authors thanks are for the support of the Atmospheric Dispersion Project (ADP) funded by the National Oceanic and Atmospheric Administration through the US Department of Commerce (Silver Springs, MD); Contract no. NA06OAR4600192. They are thankful to the anonymous reviewers for suggesting many improvements in the paper.

References

[1] S. G. Douglas, J. L. Haney, Y. H. Wei, B. Wang, and S. Beckmann, *Gulf Coast Ozone Study (GCOS) Modeling Analysis Phase III: Additional Future Year Assessments*, Systems Applications International, San Rafael, Calif, USA, 2005.

[2] A. Yerramilli, V. S. Challa, J. Indracanti et al., “Some observational and modeling studies of the atmospheric boundary layer at Mississippi Gulf Coast for air pollution dispersion assessment,” *International Journal of Environmental Research and Public Health*, vol. 5, no. 5, pp. 484–497, 2008.

[3] V. S. Challa, J. Indrcanti, J. M. Baham et al., “Sensitivity of atmospheric dispersion simulations by HYSPLIT to the meteorological predictions from a meso-scale model,” *Environmental Fluid Mechanics*, vol. 8, no. 4, pp. 367–387, 2008.

[4] V. S. Challa, J. Indracanti, M. K. Rabarison et al., “A simulation study of mesoscale coastal circulations in Mississippi Gulf coast,” *Atmospheric Research*, vol. 91, no. 1, pp. 9–25, 2009.

[5] D. W. Byun and J. K. S. Ching, Eds., “Science algorithms of the EPA Models-3 Community Multiscale Air Quality Model (CMAQ) modeling system,” Tech. Rep. EPA/600/R-99/030, US Environmental Protection Agency, Office of Research and Development, Washington, DC, USA, 1999.

[6] G. Sistla, N. Zhou, W. Hao et al., “Effects of uncertainties in meteorological inputs on urban airshed model predictions and ozone control strategies,” *Atmospheric Environment*, vol. 30, no. 12, pp. 2011–2025, 1996.

[7] Q. Mao, L. L. Gautney, T. M. Cook, M. E. Jacobs, S. N. Smith, and J. J. Kelsoe, “Numerical experiments on MM5-CMAQ sensitivity to various PBL schemes,” *Atmospheric Environment*, vol. 40, no. 17, pp. 3092–3110, 2006.

[8] Y. Zhang, P. Liu, B. Pun, and C. Seigneur, “A comprehensive performance evaluation of MM5-CMAQ for the Summer 1999 Southern Oxidants Study episode—part I: evaluation protocols, databases, and meteorological predictions,” *Atmospheric Environment*, vol. 40, no. 26, pp. 4825–4838, 2006.

[9] T. L. Otte, “The impact of nudging in the meteorological model for retrospective air quality simulations. Part I: evaluation against national observation networks,” *Journal of Applied Meteorology and Climatology*, vol. 47, no. 7, pp. 1853–1867, 2008.

[10] S. R. Hanna, “Mesoscale meteorological model evaluation techniques with emphasis on needs of air quality models,” in *Meteorological Monographs: Mesoscale Modelling of the Atmosphere*, R. A. Pielke and R. P. Pearce, Eds., vol. 25, American Meteorological Society, Boston, Mass, USA, 1994.

[11] N. L. Seaman, “Meteorological modeling for air-quality assessments,” *Atmospheric Environment*, vol. 34, no. 12–14, pp. 2231–2259, 2000.

[12] P. Jiménez, O. Jorba, R. Parra, and J. M. Baldasano, “Evaluation of MM5-EMICAT2000-CMAQ performance and sensitivity in complex terrain: high-resolution application to the northeastern Iberian Peninsula,” *Atmospheric Environment*, vol. 40, no. 26, pp. 5056–5072, 2006.

[13] J. T. McQueen, R. R. Draxler, and G. D. Rolph, “Influence of grid size and terrain resolution on wind field predictions from an operational mesoscale model,” *Journal of Applied Meteorology*, vol. 34, no. 10, pp. 2166–2181, 1995.

[14] R. A. Pielke and M. Uliasz, “Use of meteorological models as input to regional and mesoscale air quality models—limitations and strengths,” *Atmospheric Environment*, vol. 32, no. 8, pp. 1455–1466, 1998.

[15] T. T. Warner, R.-S. Sheu, J. F. Bowers, R. I. Sykes, G. C. Dodd, and D. S. Henn, “Ensemble simulations with coupled atmospheric dynamic and dispersion models: illustrating uncertainties in dosage simulations,” *Journal of Applied Meteorology*, vol. 41, no. 5, pp. 488–504, 2002.

[16] L. K. Berg and S. Zhong, “Sensitivity of MM5-simulated boundary layer characteristics to turbulence parameterizations,” *Journal of Applied Meteorology*, vol. 44, no. 9, pp. 1467–1483, 2005.

[17] D. R. Stauffer and N. L. Seaman, "Multiscale four-dimensional data assimilation," *Journal of Applied Meteorology*, vol. 33, no. 3, pp. 416–434, 1994.

[18] W. C. Skamarock, J. B. Klemp, J. Dudhia et al., "A description of the advanced research WRF version 3," NCAR Technical Note NCAR/TN-475+STR, Mesoscale and Microscale Meteorology Division, National Center for Atmospheric Research, Boulder, Colo, USA, 2008.

[19] A. Chandrasekar, C. R. Philbrick, B. Doddridge, R. Clark, and P. Georgopoulos, "A comparison study of RAMS simulations with aircraft, wind profiler, lidar, tethered balloon and RASS data over Philadelphia during a 1999 summer episode," *Atmospheric Environment*, vol. 37, no. 35, pp. 4973–4984, 2003.

[20] R. C. Gilliam, C. Hogrefe, and S. T. Rao, "New methods for evaluating meteorological models used in air quality applications," *Atmospheric Environment*, vol. 40, no. 26, pp. 5073–5086, 2006.

[21] S. R. Hanna and R. Yang, "Evaluations of mesoscale models' simulations of near-surface winds, temperature gradients, and mixing depths," *Journal of Applied Meteorology*, vol. 40, no. 6, pp. 1095–1104, 2001.

[22] G.-J. Steeneveld, J. Vilà-Guerau de Arellano, A. A. M. Holtslag, T. Mauritsen, G. Svensson, and E. I. F. de Bruijn, "Evaluation of limited-area models for the representation of the diurnal cycle and contrasting nights in CASES-99," *Journal of Applied Meteorology and Climatology*, vol. 47, no. 3, pp. 869–887, 2008.

[23] D.-L. Zhang and W.-Z. Zheng, "Diurnal cycles of surface winds and temperatures as simulated by five boundary layer parameterizations," *Journal of Applied Meteorology*, vol. 43, no. 1, pp. 157–169, 2004.

[24] D. R. Bright and S. L. Mullen, "The sensitivity of the numerical simulation of the southwest monsoon boundary layer to the choice of PBL turbulence parameterization in MM5," *Weather and Forecasting*, vol. 17, no. 1, pp. 99–114, 2002.

[25] G. A. Grell, S. E. Peckham, R. Schmitz et al., "Fully coupled "online" chemistry within the WRF model," *Atmospheric Environment*, vol. 39, no. 37, pp. 6957–6975, 2005.

[26] J. D. Fast, "Evaluation of the boundary layer characteristics and pollutants in Mexico City predicted by WRF," in *WRF/MM5 User's Workshop*, National Center for Atmospheric Research, 2005.

[27] Y. Zhang, X. M. Hu, G. W. Howell et al., "Modeling atmospheric aerosols in WRF/CHEM," in *WRF/MM5 Users's Workshop*, National Center for Atmospheric Research, June 2005.

[28] C. Misenis, X. Hu, S. Krishnan, Y. Zhang, and J. D. Fast, "Sensitivity of WRF/CHEM predictions to meteorological schemes," in *Proceedings of the 86th Annual AMS Conference and the 14th Joint Conference on the Applications of Air Pollution Meteorology with the A&WMA*, Atlanta, Ga, USA, January-February 2006.

[29] R. Borge, V. Alexandrov, J. José del Vas, J. Lumbreras, and E. Rodríguez, "A comprehensive sensitivity analysis of the WRF model for air quality applications over the Iberian Peninsula," *Atmospheric Environment*, vol. 42, no. 37, pp. 8560–8574, 2008.

[30] F. Jiang, T. Wang, T. Wang, M. Xie, and H. Zhao, "Numerical modeling of a continuous photochemical pollution episode in Hong Kong using WRF-chem," *Atmospheric Environment*, vol. 42, no. 38, pp. 8717–8727, 2008.

[31] B. De Foy, J. D. Fast, S. J. Paech et al., "Basin-scale wind transport during the MILAGRO field campaign and comparison to climatology using cluster analysis," *Atmospheric Chemistry and Physics*, vol. 8, no. 5, pp. 1209–1224, 2008.

[32] Y. Zhang, M. K. Dubey, S. C. Olsen, J. Zhen, and R. Zhang, "Comparisons of WRF/Chem simulations in Mexico City with ground-based RAMA measurements during the MILAGRO-2006 period," *Atmospheric Chemistry and Physics Discussions*, vol. 9, no. 1, pp. 1329–1377, 2009.

[33] W. R. Stockwell, P. Middleton, J. S. Chang, and X. Tang, "The second generation regional acid deposition model chemical mechanism for regional air quality modeling," *Journal of Geophysical Research*, vol. 95, no. 10, pp. 16.343–16.367, 1990.

[34] J. S. Chang, P. B. Middleton, W. R. Stockwell, F. S. Binkowski, and D. Byun, "The regional acid deposition model and engineering model," State-of-Science/Technology, Report 4, National Acid Precipitation Assessment Program, Washington, DC, USA, 1989.

[35] S. Madronich, "Photodissociation in the Atmosphere, 1, actinic flux and the effects of ground reflections and clouds," *Journal of Geophysical Research*, vol. 92, pp. 9740–9752, 1987.

[36] J. J. West, M. A. Zavala, L. T. Molina et al., "Modeling ozone photochemistry and evaluation of hydrocarbon emissions in the Mexico City metropolitan area," *Journal of Geophysical Research*, vol. 109, no. 19, Article ID D19312, 15 pages, 2004.

[37] J. D. Fast and S. Zhong, "Meteorological factors associated with inhomogeneous ozone concentrations within the Mexico City basin," *Journal of Geophysical Research*, vol. 103, no. 15, pp. 18927–18946, 1998.

[38] B. De Foy, J. R. Varela, L. T. Molina, and M. J. Molina, "Rapid ventilation of the Mexico City basin and regional fate of the urban plume," *Atmospheric Chemistry and Physics*, vol. 6, no. 8, pp. 2321–2335, 2006.

[39] Y.-L. Lin, R. D. Farley, and H. D. Orville, "Bulk parameterization of the snow field in a cloud model," *Journal of Climate & Applied Meteorology*, vol. 22, no. 6, pp. 1065–1092, 1983.

[40] M.-D. Chou and M. J. Suarez, "An efficient thermal infrared radiation parameterization for use in general circulation models," NASA Tech. Memo 104606, 1984.

[41] S.-Y. Hong, Y. Noh, and J. Dudhia, "A new vertical diffusion package with an explicit treatment of entrainment processes," *Monthly Weather Review*, vol. 134, no. 9, pp. 2318–2341, 2006.

[42] Z. I. Janjic, "The step-mountain coordinate: physical package," *Monthly Weather Review*, vol. 118, no. 7, pp. 1429–1443, 1990.

[43] Z. I. Janjic, "The surface layer in the NCEP Eta model," in *Proceedings of the 11th Conference on Numerical Weather Prediction*, pp. 354–355, American Meteorological Society, Norfolk, Va, USA, August 1996.

[44] J. E. Pleim, "A combined local and nonlocal closure model for the atmospheric boundary layer. Part I: model description and testing," *Journal of Applied Meteorology and Climatology*, vol. 46, no. 9, pp. 1383–1395, 2007.

[45] S.-Y. Hong and H.-L. Pan, "Nonlocal boundary layer vertical diffusion in a medium-range forecast model," *Monthly Weather Review*, vol. 124, no. 10, pp. 2322–2339, 1996.

[46] Z. I. Janjic, "Nonsingular Implementation of the Mellor–Yamada Level 2.5 Scheme in the NCEP Meso model," NCEP Office Note 437, 2002.

[47] J. Dudhia, "A multi-layer soil temperature model for MM5," in *Proceedings of the 6th PSU/NCAR Mesoscale Model Users' Workshop*, 1996.

[48] F. Chen and J. Dudhia, "Coupling and advanced land surface-hydrology model with the Penn State-NCAR MM5 modeling system. Part I: model implementation and sensitivity," *Monthly Weather Review*, vol. 129, no. 4, pp. 569–585, 2001.

[49] T. G. Smirnova, J. M. Brown, S. G. Benjamin, and D. Kim, "Parameterization of cold-season processes in the MAPS land-surface scheme," *Journal of Geophysical Research*, vol. 105, no. 3, pp. 4077–4086, 2000.

[50] J. E. Pleim and A. Xiu, "Development and testing of a surface flux and planetary boundary layer model for application in mesoscale models," *Journal of Applied Meteorology*, vol. 34, no. 1, pp. 16–32, 1995.

[51] A. Xiu and J. E. Pleim, "Development of a land surface model. Part I: application in a mesoscale meteorological model," *Journal of Applied Meteorology*, vol. 40, no. 2, pp. 192–209, 2001.

[52] C. J. Willmott, "Some comments on the evaluation of model performance," *Bulletin of the American Meteorological Society*, vol. 63, no. 11, pp. 1309–1313, 1982.

[53] W. A. Lyons, C. J. Tremback, and R. A. Pielke, "Applications of the regional atmospheric modeling system (RAMS) to provide input to photochemical grid models for the Lake Michigan Ozone Study (LMOS)," *Journal of Applied Meteorology*, vol. 34, no. 8, pp. 1762–1786, 1995.

[54] N. L. Seaman and S. A. Michelson, "Mesoscale meteorological structure of a high-ozone episode during the 1995 NARSTO-Northeast study," *Journal of Applied Meteorology*, vol. 39, no. 3, pp. 384–398, 2000.

[55] P. C. Shafran, N. L. Seaman, and G. A. Gayno, "Evaluation of numerical predictions of boundary layer structure during the Lake Michigan ozone study," *Journal of Applied Meteorology*, vol. 39, no. 3, pp. 412–436, 2000.

[56] W. Y. Y. Cheng and W. J. Steenburgh, "Evaluation of surface sensible weather forecasts by the WRF and the Eta Models over the western United States," *Weather and Forecasting*, vol. 20, no. 5, pp. 812–821, 2005.

[57] G. Roux, Y. Liu, L. D. Monache, R.-Y. Sheu, and T. T. Warner, "Verification of high resolution WRF-RTFDDA surface forecasts over mountains and plains," in *Proceedings of the 10th WRF Users' Workshop*, Boulder, Colo, USA, June 2009.